Since January 2020 Elsevier has created a COVID-19 resource centre with free information in English and Mandarin on the novel coronavirus COVID-19. The COVID-19 resource centre is hosted on Elsevier Connect, the company's public news and information website.

European Journal of Medicinal Chemistry 119 (2016) 300–318

Contents lists available at ScienceDirect

European Journal of Medicinal Chemistry

journal homepage: http://www.elsevier.com/locate/ejmech

Research paper

Structure-based design and synthesis of triazole-based macrocyclic inhibitors of norovirus protease: Structural, biochemical, spectroscopic, and antiviral studies

Pathum M. Weerawarna [a], Yunjeong Kim [b], Anushka C. Galasiti Kankanamalage [a], Vishnu C. Damalanka [a], Gerald H. Lushington [c], Kevin R. Alliston [a], Nurjahan Mehzabeen [d], Kevin P. Battaile [e], Scott Lovell [d], Kyeong-Ok Chang [b, **], William C. Groutas [a, *]

[a] Department of Chemistry, Wichita State University, Wichita, KS 67260, USA
[b] Department of Diagnostic Medicine & Pathobiology, College of Veterinary Medicine, Kansas State University, Manhattan, KS 66506, USA
[c] LiS Consulting, Lawrence, KS 66046, USA
[d] Protein Structure Laboratory, The University of Kansas, Lawrence, KS 66047, USA
[e] IMCA-CAT, Hauptman-Woodward Medical Research Institute, APS Argonne National Laboratory, Argonne, IL 60439, USA

ARTICLE INFO

Article history:
Received 21 January 2016
Received in revised form
4 April 2016
Accepted 6 April 2016
Available online 25 April 2016

Keywords:
Norovirus
Macrocyclic inhibitors
β-strand conformation
3CL protease

ABSTRACT

Outbreaks of acute gastroenteritis caused by noroviruses constitute a public health concern worldwide. To date, there are no approved drugs or vaccines for the management and prophylaxis of norovirus infections. A potentially effective strategy for the development of norovirus therapeutics entails the discovery of inhibitors of norovirus 3CL protease, an enzyme essential for noroviral replication. We describe herein the structure-based design of the first class of permeable, triazole-based macrocyclic inhibitors of norovirus 3C-like protease, as well as pertinent X-ray crystallographic, biochemical, spectroscopic, and antiviral studies.

Published by Elsevier Masson SAS.

1. Introduction

Noroviruses are the leading cause of foodborne illness in the U.S., accounting for >21 million infections per year and resulting in >70,000 hospitalizations and nearly 800 deaths [1–3]. They are also the primary cause of sporadic and epidemic acute gastroenteritis worldwide [4–5]. The morbidity and mortality associated with norovirus infection impacts disproportionately the elderly, immunocompromised individuals [6] and, in developing countries, children [7]. Combating noroviruses presents a major challenge because noroviruses are highly contagious, genetically diverse, environmentally stable, display prolonged and profuse viral shedding, evolve rapidly, and are capable of spreading in many different ways [8–9]. There are currently no effective vaccines or norovirus-specific antivirals for norovirus infection. Consequently, there is a pressing need for the discovery and development of small molecule therapeutics for the treatment and prophylaxis of norovirus infection [10–13].

Norovirus is an RNA virus that belongs to the *Norovirus* genus of the *Caliciviridae* family. It carries a positive sense single stranded RNA genome (7.7 Kb) that consists of three open reading frames (ORF1-3). ORF1 encodes a 200 kDa precursor polyprotein which is processed by a virus-encoded cysteine endopeptidase to generate at least six mature non-structural proteins [14–16]. Polyprotein processing by norovirus 3C-like protease (3CLpro) is vital for the replication of the virus, consequently, norovirus 3CLpro has emerged as an attractive target for the discovery and development of antiviral agents against norovirus infections [10–11,17].

Norovirus 3CLpro is a chymotrypsin-like cysteine protease with an active site consisting of the catalytic triad of Cys139, His30 and Glu54 and located in a groove that is sandwiched between a β-sheet domain and a β-barrel domain [17–21]. The β-barrel domain accounts for most of the binding interactions involved between a

* Corresponding author.
** Corresponding author.
E-mail addresses: kchang@vet.ksu.edu (K.-O. Chang), bill.groutas@wichita.edu (W.C. Groutas).

http://dx.doi.org/10.1016/j.ejmech.2016.04.013
0223-5234/Published by Elsevier Masson SAS.

peptide substrate and 3CLpro. A hallmark of norovirus 3CLpro, as well as other related 3C or 3CL viral proteases, is that its primary substrate specificity is dictated by the presence of a P_1 glutamine (and less frequently glutamic acid), at the S_1 subsite [22]. Furthermore, previous studies involving the mapping of the substrate specificity of 3CLpro have revealed that the protease prefers small hydrophobic amino acids such as a leucine residue at P_2 and that the plasticity of its S_3 subsite allows the protease to accommodate His, Gln or Glu [16,18,19].

In continuing our studies in this area [12,13,17,23], we describe herein the structure-based design of cell-permeable macrocyclic transition state inhibitors (I) and (II) (Fig. 1) of norovirus 3CLpro [23,24], as well as relevant structural, biochemical, spectroscopic, and cell-based studies.

2. Results and discussion

2.1. Inhibitor design

Inspection of crystal structures of norovirus 3CLpro with peptidyl inhibitors reveals that peptidyl inhibitors of norovirus 3CLpro bind to the enzyme via a network of backbone hydrogen bonds that mimic an antiparallel β-sheet [25,26]. Among these hydrogen bonds, the backbone NH and carbonyl O of the Ala160 residue forms two hydrogen bonds with the backbone carbonyl O and NH of the P_3 residue of the inhibitor (Fig. 2A). In addition, a third hydrogen bond exists between the backbone O of the Ala158 residue and the backbone NH of the P_1 residue of the inhibitor. This hydrogen bonding arrangement resembles the hydrogen bonding pattern found in antiparallel β-sheets and serves to correctly orient and position the inhibitor (or substrate) backbone to the active site. The hydrogen bonding associated with an antiparallel β-sheet is more feasible when an inhibitor (or substrate) binds to the active site of a protease in a β-strand conformation, the extended "saw tooth" conformation of a peptide ($\phi = -120 \pm 20^0$ and $\psi = +120 \pm 20^0$) where the backbone NHs are exposed to the environment [27]. As a consequence, the aforementioned binding mode permits proteases to universally recognize their ligands in the β-strand conformation [25,26].

Based on the forgoing, we recently reported the results of preliminary studies related to the design of triazole-based macrocyclic inhibitors of 3C and 3C-like proteases of picornavirus, norovirus and coronavirus [24]. Macrocyclization of linear peptidyl inhibitors was accomplished by tethering the P_1 and P_3 residues of the linear inhibitor by a suitable linker, thereby pre-organizing the macrocycle in a β-strand conformation prior to binding to the enzyme active site (Fig. 2B) [27,28]. This approach results in the formation of a pre-organized and semi-rigid entity that displays the amino acid side chains in a well-defined vector relationship for optimal binding and enhances the affinity of the inhibitor to the target enzyme by minimizing the entropy loss upon binding. Additional potential advantages of macrocyclic inhibitors include high stability to metabolizing enzymes, high selectivity and, frequently, increased cellular permeability [29–32]. We describe herein the structure-based design of macrocyclic inhibitors of norovirus 3CLpro where the side chain of the P_1 Gln primary substrate specificity residue is tethered to the P_3 residue via a triazole linker to yield macrocycles (I) (Fig. 1) and explore the effect of ring size on conformation and its impact on pharmacological activity using high field NMR and X-ray crystallographic studies. We also report the first examples of macrocyclic inhibitors of norovirus 3CLpro that are cellurarly permeable.

2.2. Chemistry

The synthesis of macrocyclic compounds **1**–**11** (Table 1) was accomplished by first constructing key intermediates **15a**–**c**, **18a**–**e**, **19a**–**e**, and **20a**–**b** using well-established methodologies (Scheme 1). The commercially available N-Boc protected L-propargylglycine was reacted with L-leucine methylester, L-cyclohexylalanine methyl ester or L-phenylalanine methyl ester, in the presence of EDCI and HOBt to provide the corresponding dipeptide

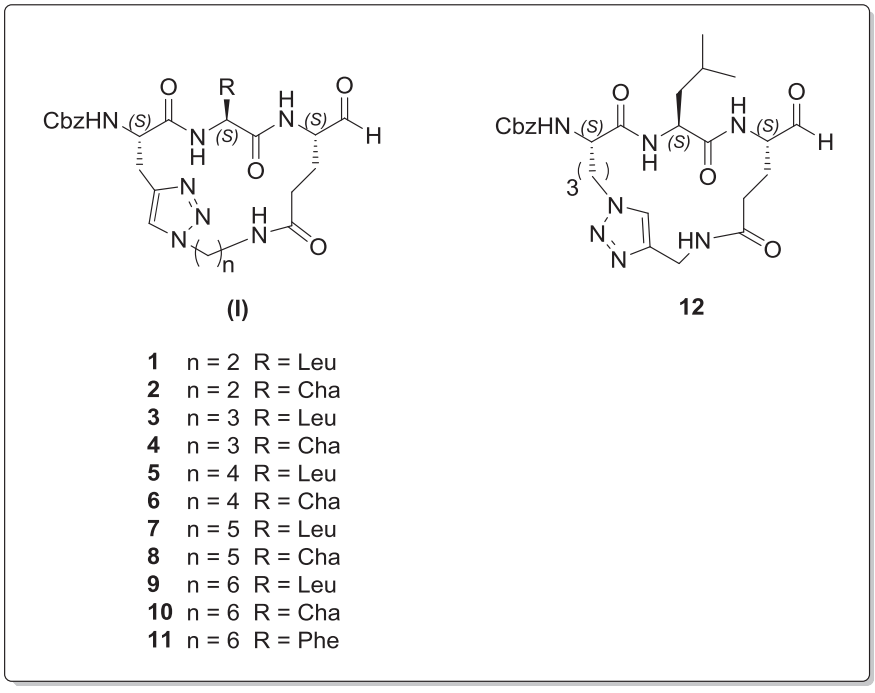

Fig. 1. General structure of macrocyclic inhibitor (I).

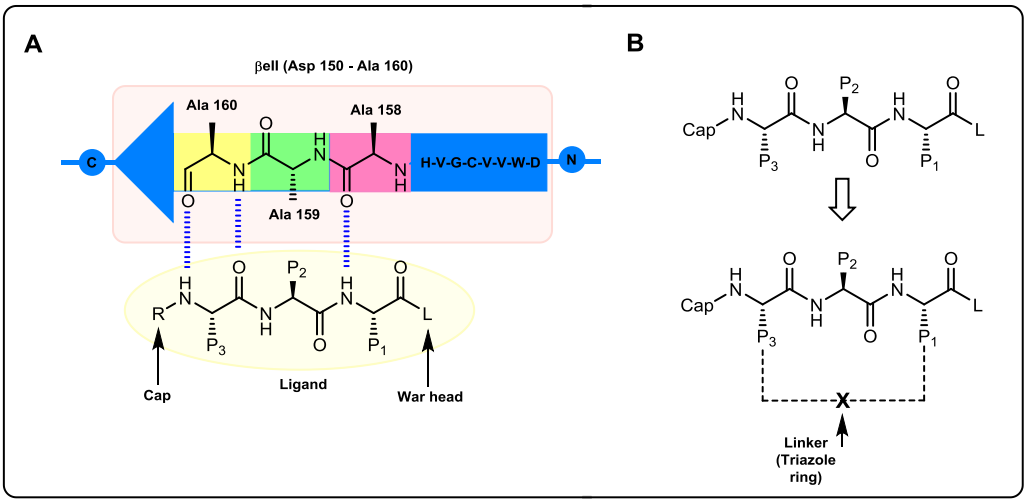

Fig. 2. A) Schematic representation of antiparallel β-sheet like hydrogen bonding between NV 3CLpro and the tripeptidyl inhibitor. B) Macrocyclization of the tripeptidyl inhibitor by connecting the P_1 and P_3 residues.

Table 1
Activity of compounds 1–11 against norovirus 3CL protease and norovirus cell-based replicon cells.

Compound	R	m	n	Ring size	IC_{50}(μM)	EC_{50} (μM)	CC_{50}(μM)
1	Isobutyl	1	2	17	1.6	53.2	>100
2	Cyclohexyl	1	2	17	2.9	25.5	>100
3	Isobutyl	1	3	18	2.4	81.5	>100
4	Cyclohexyl	1	3	18	1.6	16.1	>100
5	Isobutyl	1	4	19	6.4	46.3	>100
6	Cyclohexyl	1	4	19	1.4	30.5	>100
7	Isobutyl	1	5	20	3.7	6.2	>100
8	Cyclohexyl	1	5	20	24.5	3.8	>100
9	Isobutyl	1	6	21	4.1	42.1	>100
10	Cyclohexyl	1	6	21	6.1	88.3	>100
11	Phenyl	1	6	21	36.5	29.5	>100

esters. Deblocking of the resulting esters was accomplished by treatment with 4 M HCl in dioxane. The resulting amine hydrochlorides were reacted with benzylchloroformate followed by LiOH to yield the corresponding N-Cbz protected dipeptide acid intermediates **15a**–**c**. Preparation of the HCl salts of amino azides **18a**–**e** was effected by sequential reaction of commercially available N-Boc protected amino alcohols with methanesulfonyl chloride and sodium azide followed by deprotection with 4 M HCl in dioxane. Coupling of N-Boc protected glutamic acid with the corresponding HCl salts of amino azides **18a**–**e** in the presence of EDCI and HOBt gave intermediates **19a**–**e**, in good yields.

The macrocyclization step was effected in two different ways. Specifically, the synthesis of macrocycles **2**–**3** entailed click chemistry-mediated macrocyclization using intermediates **15a**–**c** and **20a**–**b** (Scheme 2), while compounds **1** and **4**–**11** were obtained through macrolactamization starting with key intermediates **15a**–**c** and **19a**–**e** (Scheme 3). In general, the macrolactamization methodology was found to be superior, particularly in terms of ease of purification of the resultant cyclized products. Intermediates **15a** and **20a**–**b** were coupled in the presence of EDCI and HOBt to yield the corresponding linear precursors **24a** and **24b** of the macrocyclic esters **25a** and **25b**. Intramolecular click reactions of the linear precursors **24a**–**b** were carried out using a CuI/DBU mixture in dichloromethane under a nitrogen atmosphere at room temperature for 24 h to provide macrocyclic esters **25a**–**b** in fairly good yields (45–50%). Intermediates **15a**–**c** and **19a**–**e** were coupled using intermolecular click reaction in the presence of $CuSO_4$ and sodium ascorbate in THF/H_2O solution to obtain the corresponding linear precursors **27a**–**i** of macrocyclic esters **28a**–**i**. Macrolactamization of compounds **27a**–**i** was carried out using EDCI and HOBt in DMF at room temperature for 24 h to yield macrocyclic esters **28a**–**i** in good yields (~60%). In both cyclization methods, the dilution factor of the reaction mixture was critical in controlling the intramolecular cyclization reaction over the intermolecular reaction. Reduction of macrocyclic esters using $LiBH_4$ followed by Dess–Martin periodinane oxidation provided the corresponding macrocyclic aldehydes **1**–**11** in fairly good yields (~50%).

The orientation of the triazole ring and its effect on pharmacological activity and conformation was probed by synthesizing macrocycle **12**, via intermediates **21** and **23**, as illustrated in Scheme 4. The acyclic variant of macrocycle **3** was synthesized according to Scheme 5 in order to determine the effect of macrocyclization on antiviral activity. As dictated by the primary substrate specificity of norovirus 3CLpro, the P_1 Gln residue remained invariant in all synthesized inhibitors. Furthermore, norovirus 3CLpro prefers a P_2 Leu or Cha [12,23a-c], consequently, the convergent nature of the synthetic plan allowed for variations in the P_2 residue via the judicious selection of appropriate natural or unnatural amino acid esters, thereby permitting the targeting of related viral proteases in the and *Coronaviridae* families.

2.3. Biochemical studies

The inhibitory activity of compounds **1**–**12** against norovirus 3CLpro *in vitro* and norovirus in a cell-based replicon system was evaluated as previously described [12,13] and the results are summarized in Table 1.

2.4. X-ray crystallography

In order to establish the precise mechanism of action of inhibitors (I) and gain insight and understanding into the structural determinants that impact potency and permeability that can be used to facilitate the structure-guided optimization of pharmacological activity, high-resolution X-ray crystal structures of NV 3CLpro with bound inhibitors **1**, **3**, and **10** were determined. Attempts to obtain crystal structures of permeable inhibitors **7** and **8**

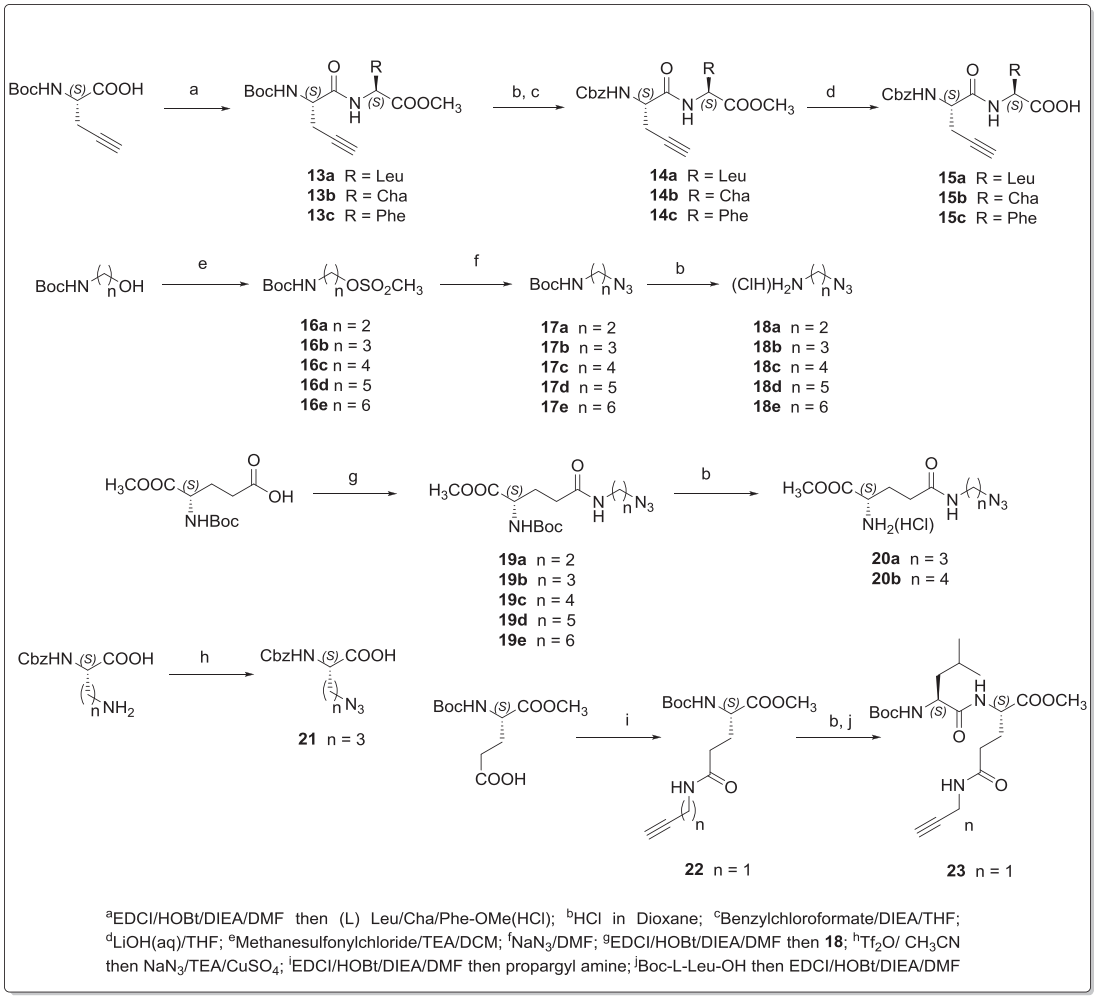

Scheme 1. Synthesis of key intermediates.

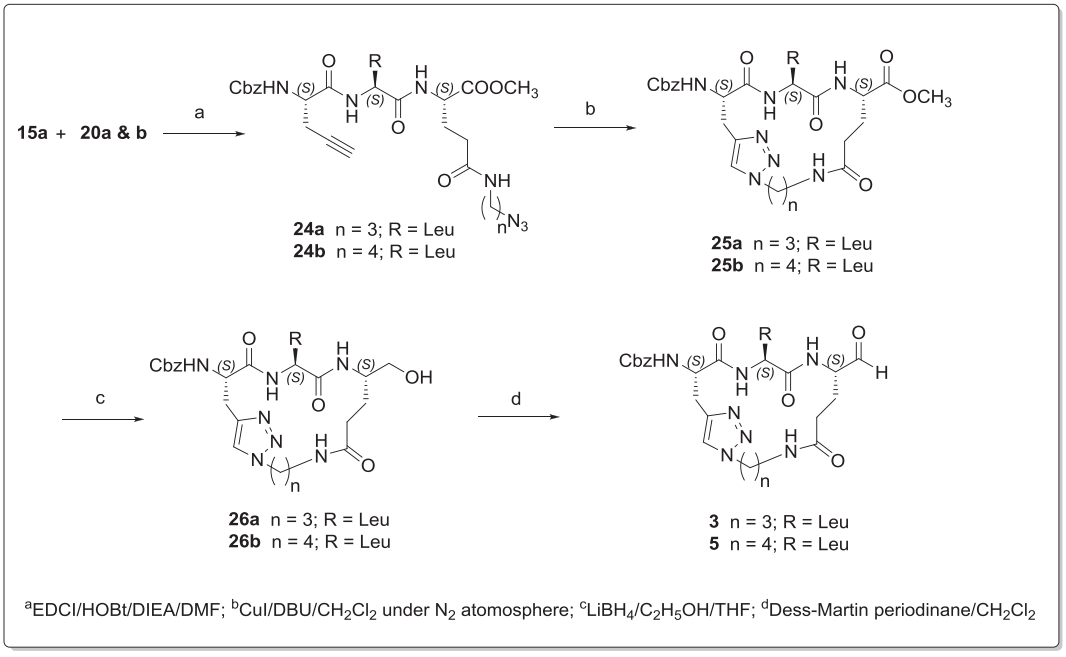

Scheme 2. Synthesis of macrocyclic aldehydes via intramolecular Huisgen cycloaddtion.

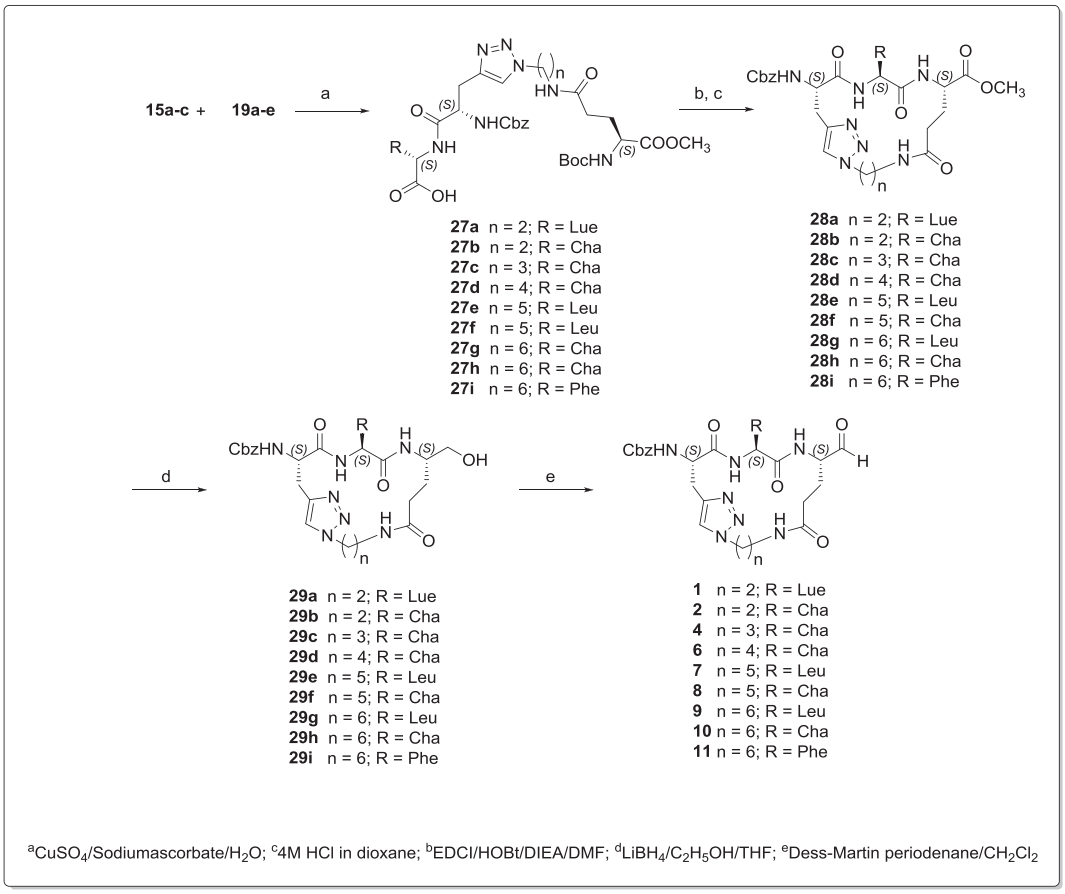

Scheme 3. Synthesis of macrocyclic aldehydes via macrolactamization.

were unsuccessful, precluding a structural comparison between the permeable and non-permeable macrocyclic inhibitors that might perhaps illuminate the structural determinants responsible for the observed differences in potency and cellular permeability.

Examination of the active site revealed the presence of an antiparallel β-sheet-like hydrogen bonding network associated with the backbone of all three inhibitors, covalently bound to the catalytic Cys139 residue (Fig. 3). The coordinates of the Ramachandran plot (see Fig. S8 in Supporting information) of six ϕ and ψ angle pairs of the corresponding P_2 and P_3 residues, extracted from the X-ray crystal structures, lie in the upper left quadrant of the plot, indicating that bound inhibitors **1**, **3**, and **10** assume an extended β-strand conformation. The pseudo ϕ angles of the P_1 residue covalently bound to the Cys139 residue range from −129.5° to −137.8°. The electron density maps for the three bound inhibitors are shown in Fig. 4A–C. As expected, the backbones of all three inhibitors are structurally more rigid compared to the atoms forming the macrocyclic linker, which is more flexible. This is evident from an analysis of the *B*-factors for the inhibitors in each structure, which are slightly lower in the backbone region as shown in the right panels of Fig. 4A–C. The electron density for the "cap" phenyl ring was not observed for **1** and **3** due to disorder and could not be modeled, while inhibitor **10** has somewhat weak electron density that permitted modeling of the phenyl ring. The triazole ring of inhibitor **3** has reasonable electron density, however, it is more disordered and its exact orientation is not clearly discernible (Fig. 4).

Perusal of Table 1 indicates that, with the exception of compounds **8** and **11**, the rest of the compounds displayed low micromolar IC_{50} values. The observed degree of inhibition prompted us to delineate the structural determinants associated with binding in order to gain insight and understanding into the relative potency of the inhibitors. Toward that end, superposition with GESAMT [33] of the high-resolution X-ray crystal structure of the NV 3CLpro:**10** complex (largest ring size) with the NV 3CLPro:**1** complex (smallest ring size) shows that the enzyme structures in both complexes are similar, with an RMSD between Cα atoms of 0.76 Å (167 residues), except for the flexible loop spanning Lys121 to Glu140 (Fig. 5A). The binding of inhibitor **10** (larger ring size) to the active site is accompanied by the movement of the flexible loop away from the inhibitor resulting in the loss of a hydrogen bond between the P_1 side chain (Gln C═O) of the inhibitor with Thr134 (backbone NH) which forms the S_1 pocket. His157, which is the other constituent of the S_1 pocket but is not a part of the flexible loop, maintains a hydrogen bond interaction with the P_1 Gln C═O (Fig. 5B). It should be noted that the interaction of NV 3CLpro with acyclic dipeptidyl and tripeptidyl inhibitors involves the formation of two crucial hydrogen bonds between the carbonyl oxygen of the glutamine surrogate C═O in the inhibitor and the Thr134 and His157 residues [12]. These two hydrogen bonding interactions, as well as the flexible backbone of the T123-G133 loop [34], appear to play a critical role in enzyme-substrate recognition and are conserved in all norovirus proteases. Thus, in the NV 3CLpro:**1** complex, the movement of the flexible loop and the shorter linker length of the inhibitor which positions the carbonyl oxygen of the P_1 Gln side chain away from His157 and Thr134, results in the loss

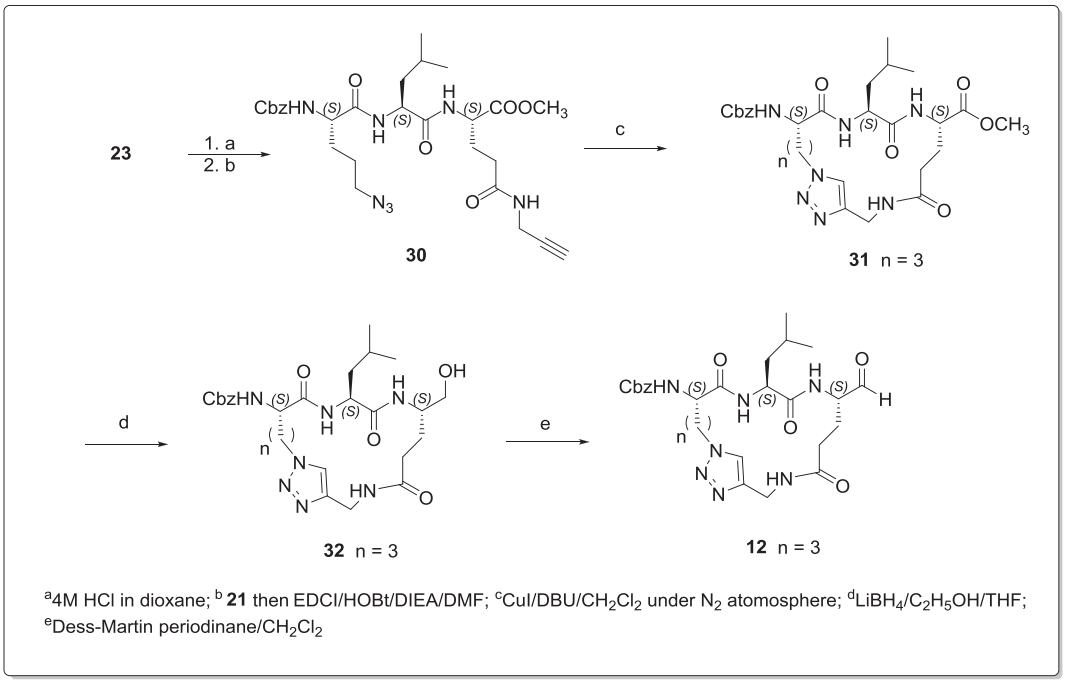

Scheme 4. Synthesis of macrocyclic aldehyde **12**.

of the Thr134 P_1 Gln C═O hydrogen bond (Fig. 5C). Conversely, the binding of inhibitor **1** allows the flexible loop to move closer to the inhibitor such that a contact can be formed (3.3 Å) between Pro136 and the carbonyl oxygen of the warhead (Fig. 5B).

The compact nature of the inhibitor positions the NH group of the P_1 Gln side chain within hydrogen bonding distance (3.2 Å) of the carbonyl oxygen of the Ala160 residue (see Fig. S1 in Supporting information for distance information related to the hydrogen bonds). The subtle structural shifts associated with the P1 Gln side chain may account for the lower inhibitory activity observed with this series of macrocyclic triazole compounds, as compared to previously reported triazole-based macrocyclic calpain inhibitors [35] specifically and macrocyclic inhibitors generally [29–31]. In the former case, potency is solely dependent on the combined effect of hydrophobic interactions and the network of hydrogen bonding interactions between the inhibitor backbone and the enzyme active site which is facilitated by the β-strand conformation of the inhibitor.

The enhancement in the IC_{50} values associated with the replacement of the P_2 isobutyl side chain with a cyclohexyl group observed with linear dipeptidyl inhibitors [12] is diminished in compound **10** (IC_{50} 6.1 μM) and is partly due to the loss of the key hydrogen bonding interaction with Thr134, as revealed by the X-ray crystal structure and the larger flexible ring (see discussion of NMR studies). On the other hand, as mentioned above, the compact, rigid ring structure and the additional hydrogen bond with Ala160, discernible from the X-ray crystal structure, may account for the 4-fold decrease in the IC_{50} value (1.6 μM) of compound **1** as compared to compound **10**. The *in vitro* inhibitory activity of compounds **1** and **3** which form the same number of direct hydrogen bonds with the enzyme (7 hydrogen bonds) was found to be 1.6 μM and 2.4 μM, respectively. Interestingly, compound **34,** the acyclic variant of compound **3,** was devoid of any inhibitory activity. Finally, the 18-membered macrocycle **12** (Fig. 1) in which the triazole ring was constructed in a reverse fashion and presumably assumes a different orientation than inhibitors **1**–**11**, was effective against

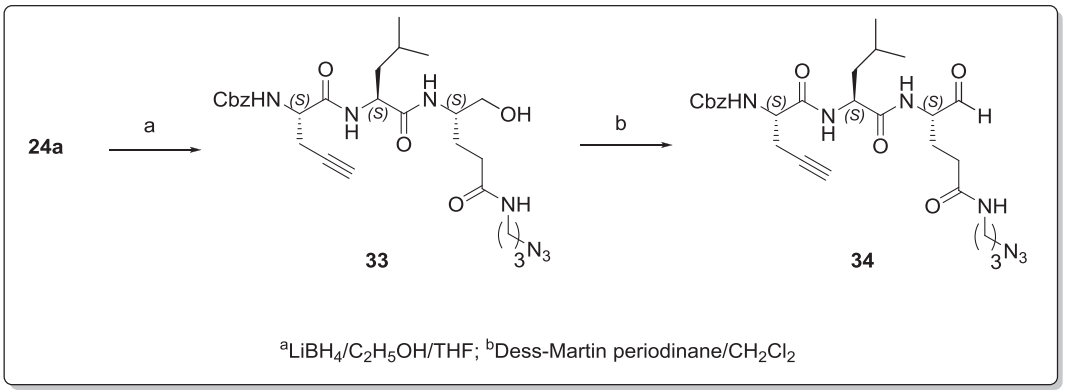

Scheme 5. Synthesis of linear aldehyde **34**.

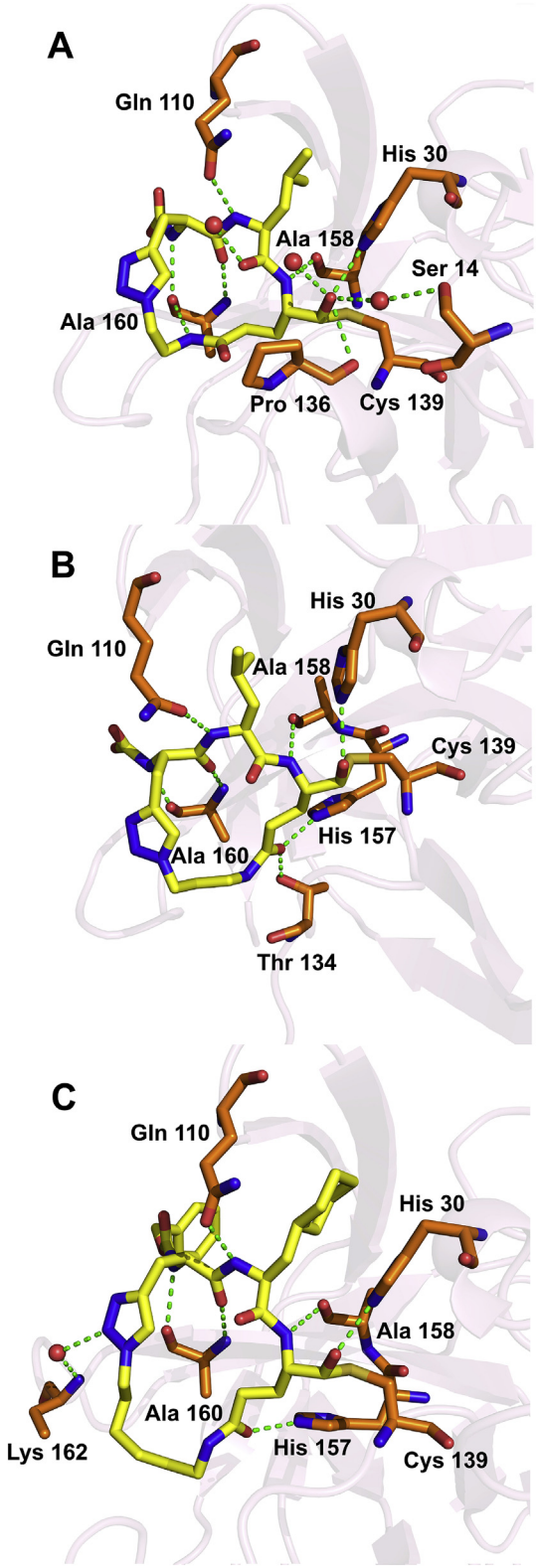

Fig. 3. Hydrogen bonding interactions derived from co-crystal structures of three inhibitors bound to NV 3CLpro. A) NV 3CLpro:**1** complex. B) NV 3CLpro:**3** complex. C) NV 3CLpro:**10** complex.

both 3CLpro and norovirus in replicon cells having IC_{50} and EC_{50} values 15.5 μM and 8.5 μM, respectively.

In summary, the interaction of macrocyclic inhibitors (I) with NV 3CLpro induces conformational changes in the flexible loop and active site of the enzyme which are dependent on macrocycle ring size and structure. These changes result in sub-optimal angles and distances in forming the critical intermolecular hydrogen bonds between the P1 Gln side chain and the active site His157 and Thr134 residues, consequently, maximal binding potency and effective compensation for the energy penalty required to desolvate the molecule, are not attained.

2.5. NMR studies

In order to gain further insight into the solution conformation and binding of the synthesized macrocyclic inhibitors, as well as confirm the absence of alternate structures, NMR studies were carried out using the precursor cyclic esters. Assignment of the proton resonances was done using ^{1}H, COSY, ROESY and HMBC spectral details. The ROESY spectra of the compounds show $H_{i\alpha}$ to NH ($i + 1$) type correlation, where the Gln and Leu NH show correlation to the Leu Hα and carbamate Hα, respectively (see Figs. S1–S5 in Supporting information). This observation is indicative of a prearranged structure within the macrocycle [28]. The temperature dependence of amide NH chemical shifts experiments were performed using compounds **28a** (ring size: 17), **28e** (ring size: 20) and **28g** (ring size: 21), revealing important information about the solution structures of the macrocycles. Solvent shielded NH protons typically have $\Delta\delta/T$ values less than 4 ppb/K while solvent exposed NH protons have $\Delta\delta/T$ values greater than 4 ppb/K [28]. According to the results, the Gln, Leu, and propargylglycine NH protons have $\Delta\delta/T$ values greater than 4 ppb/K in all cases (Table 3). At larger ring sizes, the carbamate NH shows a higher temperature dependence (−7.0 and 6.4 ppb/K for ring sizes 20 and 21, respectively), indicating greater solvent exposure. However, for smaller ring size it shows comparatively low temperature dependence (4.2 ppb/K at 17 ring size), indicating less solvent exposure. This is further supported by the observed line broadening of the carbamate NH proton at elevated temperatures for compounds **28e** and **28g**, and the lower line broadening observed for **28a** (Fig. S6 in Supporting information). Previous studies have shown that amide signals exchanging with water impurity present in DMSO solvent show considerable broadening of the line width at elevated temperatures due to the enhanced exchange rate at higher temperatures [28]. At smaller ring size, all three NH protons show less temperature dependence, indicating solvent shielding which is partly due to the compact nature of the compound. The absence of very low temperature dependent NH protons (~2 ppb/K) would appear to rule out the presence of alternative turn structures, such as γ-turns. Finally, the conformations of the peptide backbone of macrocycles **28a** and **28h** were determined based on 1D $^3J_{NH\text{-}CH\alpha}$ coupling constants (Table 4). The coupling constant $^3J_{NH\text{-}CH\alpha}$ correlates with the dihedral angle (ψ) according to the Karplus equation [28]. For unstructured random coil conformations the coupling constant is around 7 Hz while unusually high coupling constants (>9 Hz) are observed for well-structured β-strands. According to the results shown in Table 4, the expected β-strand conformation was observed only for the 17-membered ring.

3. Conclusion

The studies described herein demonstrate the feasibility of generating cell-permeable triazole-based macrocyclic inhibitors of norovirus 3CL protease. Valuable insights into the mechanism of action, conformation, and pharmacological activity were gained using an array of structural, spectroscopic, and antiviral techniques and methodologies. The interaction of inhibitor (I) with NV

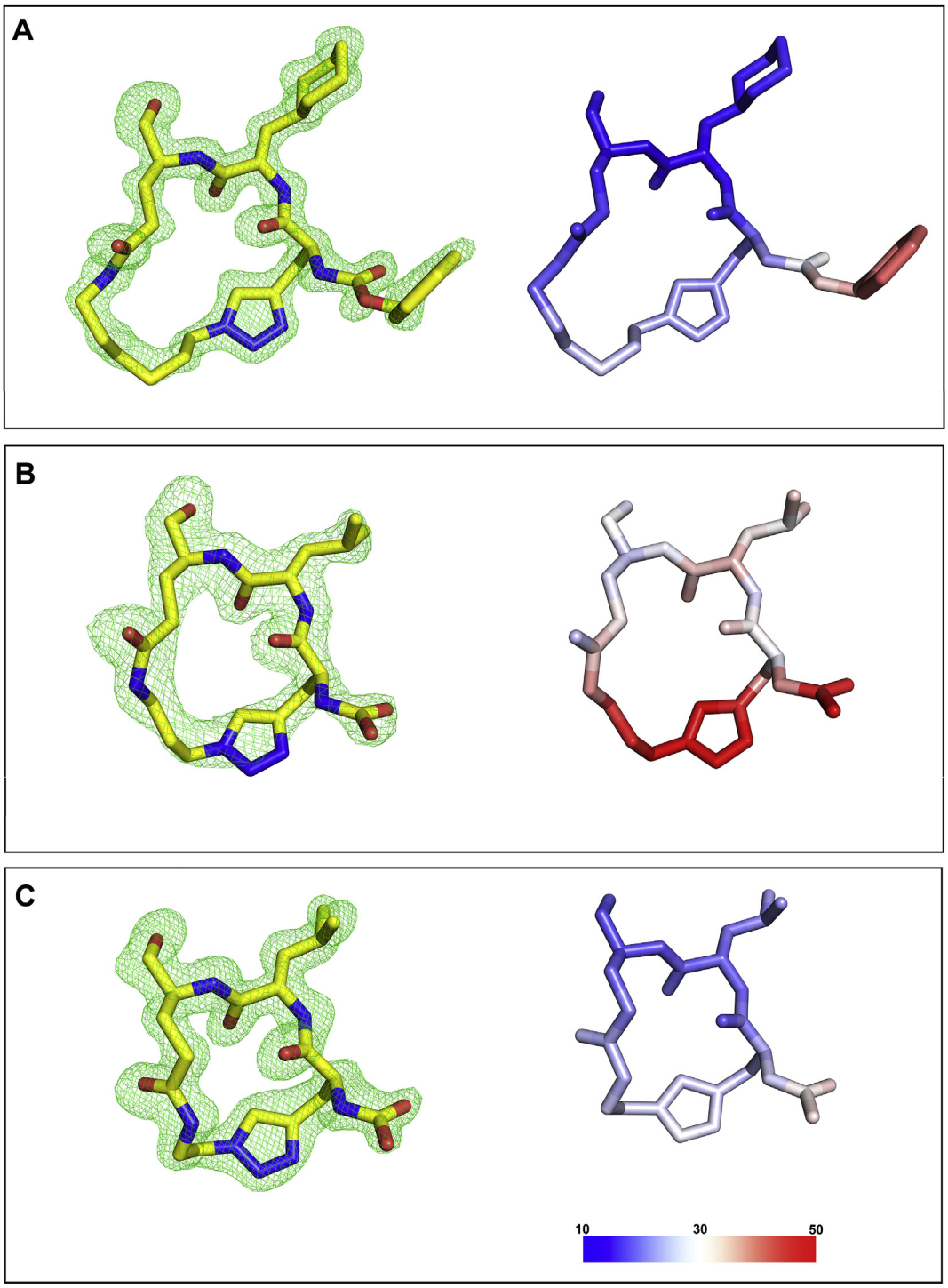

Fig. 4. F_o–F_c electron density maps contoured at 3σ for three inhibitors (left) and same inhibitors colored according to *B*-factors (right) (minimum = 10, maximum = 50). A) NV3CLpro:**10** complex. B) NV 3CLpro:**3** complex. C) NV 3CLpro:**1** complex.

3CLpro results in subtle structural shifts in the active site topography that impair hydrogen bonding interactions between the P1 Gln residue in the inhibitor and key amino acid residues and contribute to lower pharmacological activity. The results of ongoing studies are likely to illuminate further the interplay of ring size, conformation, and cellular permeability, and will reported in due course.

4. Experimental section

4.1. General

Reagents and dry solvents were purchased from various chemical suppliers (Aldrich, Acros Organics, ChemImpex, TCI America, and Bachem) and were used as obtained. Silica gel (230–450 mesh) used for flash chromatography was purchased from Sorbent

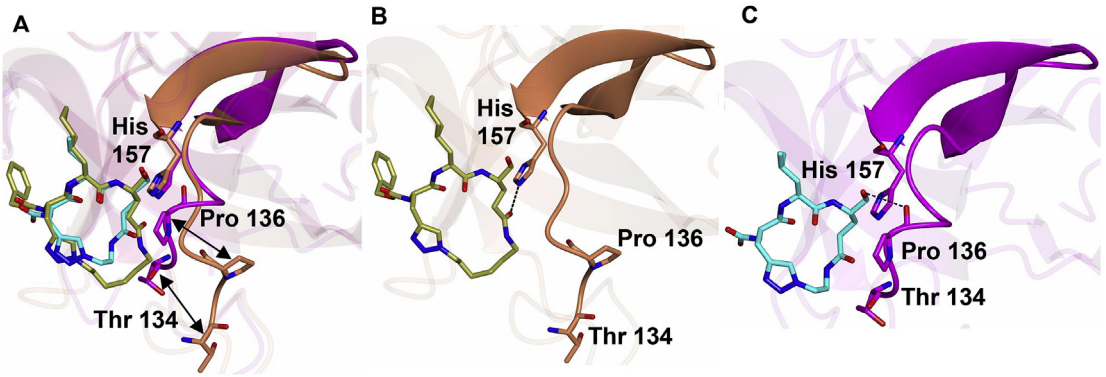

Fig. 5. Comparison of the high-resolution X-ray crystal structures of the NV 3CLpro:**10** (orange) and NV 3CLpro:**1** (magenta) complexes. Inhibitors **10** and **1** are colored yellow and cyan respectively. A) Superposition NV 3CLpro:**10** and NV 3CLpro:**1** highlighting the differences in the region spanning Thr 134 to His 157. The arrows indicate that conformation differences in Thr 134/Pro 136 in the flexible loop region. B and C) Differences in hydrogen bond/close contacts (dashed lines) in the flexible loop region for 3CLpro:**10** and NV 3CLpro:**1** respectively. (For interpretation of the references to colour in this figure legend, the reader is referred to the web version of this article.)

Table 2
Crystallographic data for norovirus 3CL protease:Inhibitor structures.

	NV 3CLpro:1	NV 3CLpro:3	NV 3CLpro:10
Data collection			
Unit-cell parameters (Å, °)	$a = 65.84$, $b = 39.28$, $c = 61.32$, $\beta = 118.7$	$a = 38.10$, $b = 48.77$, $c = 53.08$ $\alpha = 94.0$, $\beta = 109.5$, $\gamma = 101.3$	$a = 66.67$, $b = 37.16$, $c = 61.86$, $\beta = 110.0$
Space group	*C*2	*P*1	*C*2
Resolution (Å)[a]	33.24–1.20 (1.22–1.20)	37.01–1.95 (2.00–1.95)	32.63–1.20 (1.22–1.20)
Wavelength (Å)	1.0000	1.0000	1.0000
Temperature (K)	100	100	100
Observed reflections	147,835	43,724	264,169
Unique reflections	44,826	24,256	42,941
<I/σ(I)>[a]	14.1 (2.1)	8.0 (1.7)	16.3 (1.9)
Completeness (%)[a]	96.7 (94.2)	95.2 (94.0)	96.5 (93.7)
Multiplicity[a]	3.3 (3.2)	1.8 (1.8)	5.7 (3.6)
R_{merge} (%)[a,b]	3.7 (58.0)	4.6 (44.2)	5.8 (78.7)
R_{meas} (%)[a,d]	4.4 (69.4)	6.5 (62.5)	6.3 (92.4)
R_{pim} (%)[a,d]	2.4 (37.7)	4.6 (44.2)	2.5 (47.6)
$CC_{1/2}$[a,e]	0.999 (0.758)	0.997 (0.755)	0.999 (0.688)
Refinement			
Resolution (Å)[a]	31.18–1.20	37.01–1.95	31.96–1.20
Reflections (working/test)[a]	42,608/2205	22,998/1244	40,906/2020
R_{factor}/R_{free} (%)[a,c]	13.8/16.1	18.3/21.9	13.7/16.5
No. of atoms (protein/ligand/water)	1292/32/165	2395/33/94	1295/46/170
Model quality			
R.m.s deviations			
Bond lengths (Å)	0.010	0.011	0.009
Bond angles (°)	1.109	1.136	1.087
Average B-factor (Å[b]*)*			
All Atoms	20.1	38.6	19.0
Protein	18.5	38.6	17.4
Ligand	24.1	38.3	22.7
Water	32.3	38.9	30.5
Coordinate error (maximum likelihood) (Å)	0.12	0.21	0.10
Ramachandran plot			
Most favored (%)	98.9	97.5	97.2
Additionally allowed (%)	1.1	2.5	2.8

[a] Values in parenthesis are for the highest resolution shell.
[b] $R_{merge} = \Sigma_{hkl}\Sigma_i |I_i(hkl) - \langle I(hkl)\rangle| / \Sigma_{hkl}\Sigma_i I_i(hkl)$, where $I_i(hkl)$ is the intensity measured for the *i*th reflection and $\langle I(hkl)\rangle$ is the average intensity of all reflections with indices hkl.
[c] $R_{factor} = \Sigma_{hkl} ||F_{obs}(hkl)| - |F_{calc}(hkl)|| / \Sigma_{hkl} |F_{obs}(hkl)|$; Rfree is calculated in an identical manner using 5% of randomly selected reflections that were not included in the refinement.
[d] R_{meas} = redundancy-independent (multiplicity-weighted) R_{merge} [46]. R_{pim} = precision-indicating (multiplicity-weighted) R_{merge} [47,48].
[e] $CC_{1/2}$ is the correlation coefficient of the mean intensities between two random half-sets of data [49–50].

Technologies (Atlanta, GA). Thin layer chromatography was performed using Analtech silica gel plates. Visualization was accomplished using UV light and/or iodine. The ^{1}H NMR were recorded in $CDCl_3$ or DMSO-d_6 using a Varian XL-400 spectrometer and are reported relative to TMS ($\delta_H = 0.00$ ppm). Chemical shifts are reported in ppm and spin multiplicities are represented by the following signals: s (singlet), d (doublet), dd (doublet of doublets), t (triplet), q (quartet) and m (multiplet). Melting points were

Table 3
Temperature dependence of amide hydrogens.

Compound	Ring size	Temperature dependence of NH ($\Delta\delta/T$ *ppb/K*)		
		Glutamine (P_1)	Leucine (P_2)	Carbamate (P_3)
28a	17	−4.5	−4.9	−4.2
28e	20	−5.5	−5.0	−7.0
28g	21	−4.5	−5.7	−6.4

Table 4
$^{3J}NH\text{-}CH_{\alpha}$ coupling constant values of precursor macrocyclic esters.

Compound	$^{3}J_{NH\text{-}CH\alpha}$ (Hz)				Ring size	β-strand[a]	IC_{50}(μM)[b]
	P_1	P_2		P_3			
	Gln	Leu	Cha	Cab			
28a	9.76	4.69	–	8.20	17	Yes	1.2
28b	9.46	–	4.41	8.60	17	Yes	2.9
25a	8.20	7.42	–	7.03	18	No	2.4
28c	8.20	–	7.42	7.81	18	No	1.6
25b	7.81	7.42	–	7.81	19	No	6.4
28d	7.42	–	7.72	7.81	19	No	1.4
28e	7.42	7.81	–	8.6	20	No	3.7
28f	6.64	–	7.81	ND[c]	20	No	24.5
28g	7.81	8.2	–	5.86	21	No	4.1
28h	7.63	–	7.63	6.1	21	No	6.1

[a] β-strand conformation with respect to P_1 and P_3 residues.
[b] IC_{50} values of corresponding aldehydes of the precursor esters.
[c] Not detected due to overlapping resonances.

recorded on a Mel-Temp apparatus and are uncorrected. High resolution mass spectrometry (HRMS) was performed at the University of Kansas Mass Spectrometry lab using an LCT Premier mass spectrometer (Waters, Milford, MA) equipped with a time of flight mass analyzer and an electrospray ion source. The purity of the compounds was established using HPLC and was >95%.

4.1.1. General procedure A. Peptide coupling reaction

To a solution of N-protected amino acid derivative (1.0 eq) in dry DMF was added EDCI (1.22 eq), HOBt (eq) and the reaction mixture was stirred at room temperature for 40 min (Solution A). In the meantime, O-protected amino acid/amine (1.0 eq) in dry DMF kept at 0 °C was added DIEA (4 eq) and stirred for 25 min (Solution B). After that Solution B was transferred to Solution A and stirred overnight at room temperature. The solvent was removed on the rotary evaporator and residue was taken up with ethyl acetate, washed sequentially with saturated sodium bicarbonate, 5% HCl and brine. The organic layer was dried over anhydrous sodium sulfate, filtered and the solvent was removed on the rotary evaporator. See individual experiments for details.

4.1.2. General procedure B. Hydrolysis of methyl esters

A solution of compound methyl ester (1.0 eq) in dry THF kept in an ice bath was treated with a solution of 1 M lithium hydroxide (3.5 eq) and stirred for 4 h at 0 °C until the starting material disappeared (as shown by TLC). The solvent was removed and the residue was diluted with water. The pH of the aqueous solution was adjusted to ~2 with 5% HCl and acidified solution was extracted with ethyl acetate and washed with brine. Organic extract was dried using anhydrous sodium sulfate, filtered and solvent was removed on the rotary evaporator. For details, see individual experiments.

4.1.3. General procedure C. Removal of N-Boc protection

A solution of *N*-Boc protected compound (1.0 eq) in dry DCM was treated with 4 M HCl in dioxane (10 eq) and stirred at room temperature for 3 h while monitoring the disappearance of the starting material by TLC. Solvent was removed on the rotary evaporator, residue was treated with ether and concentrated. See individual experiments for details.

4.1.4. General procedure D. Conversion of N-Boc protected alcohol to mesylate

To a solution of *N*-Boc protected alcohol (60 mmol) and TEA (60 mmol) in dry DCM (100 mL) kept in an ice bath (0 °C) was slowly added methane sulfonyl chloride (60 mmol)) and reaction mixture was stirred for 30 min at 0 °C. The ice bath was removed and reaction mixture was further allowed to stir at room temperature for 5 h (Completion of the reaction was monitored by TLC). Then water (50 mL) was added with stirring, the resulting solution was transferred to a reparatory funnel, organic layer was separated and aqueous layer was extracted with DCM (2 × 75 mL). The combined organic layers were washed with brine (50 mL) dried over anhydrous sodium sulfate and concentrated on rotary evaporator. See individual experiments for more details.

4.1.5. General procedure E. Conversion of N-Boc protected mesylate to azide

To a solution of compound *N*-Boc protected mesylate (60 mmol) in dry DMF (150 mL) was added in small portions NaN_3 (180 mmol) with stirring over 30 min. Resulting solution was heated to 50 °C for 1 h and it was further allowed to react overnight at room temperature. Then water (50 mL) was added with stirring, solvent was removed and residue was extracted with ethyl acetate (2 × 175 mL). The combined organic layers were washed sequentially with water (2 × 50 mL), brine (2 × 50 mL) and solvent was dried over anhydrous sodium sulfate and evaporated on rotary evaporator. See individual experiments for more details.

4.1.6. General procedure F. Intermolecular click reactions

To a stirred solution of alkyne (5 mmol) in a mixture of water and THF (1:1, 25 mL) was added corresponding azide (5 mmol) followed by addition of sodium ascorbate (0.5 mmol) and $CuSO_4.5H_2O$ (0.25 mmol). Resulting solution was further allowed to react 20 h at room temperature. See individual experiments for more details.

4.1.7. General procedure G. Intramolecular click reaction

To a solution of macrocycle precursor (0.512 mmol) in dry DCM (1.2 M) under N_2 atmosphere, was added DBU (1.53 mmol) while solution was stirring vigorously at room temperature. After 15 min Cu(I)Br (0.512 mmol) was added and reaction mixture was stirred for 12 h at room temperature. After that it was quenched by adding 3 M HCl (100 mL), aqueous layer was separated and extracted with DCM (2 × 500 mL). The combined organic layers were washed sequentially with water (300 mL), brine (300 mL), dried over anhydrous sodium sulfate, filtered and concentrated on rotary evaporator. See individual experiments for more details.

4.1.8. General procedure H. Macrolactamization reaction

To a solution of macrocycle precursor (1 mmol) in dry DMF (2 M) was added DIEA (4 mmol) and stirred for 30 min. After that, was added EDCI (1.25 mmol) followed by HOBt (1.25 mmol) and resulting solution was stirred for 20 h at room temperature. The solvent was removed on the rotary evaporator and residue was taken up with DCM, washed sequentially with saturated sodium bicarbonate, 5% HCl and brine. The organic layer was dried over anhydrous sodium sulfate, filtered and the solvent was removed on the rotary evaporator. See individual experiments for details.

4.1.9. General procedure I. Reduction of macrocycle esters

To a solution of compound macrocycle ester (1 mmol) in dry THF (6 mL) was added a solution of 2 M $LiBH_4$ (3.0 mmol) drop wise followed by drop wise addition of absolute ethanol (11 mL) and was stirred at room temperature for 16 h while monitoring the disappearance of the starting material by TLC. After that solvent was removed on the rotary evaporator and residue was partitioned between ethyl acetate and 1 M $KHSO_4$. The aqueous phase was extracted twice more chloroform and each organic extract was washed with brine separately, dried over anhydrous sodium sulfate and evaporated to give corresponding alcohol. See individual experiments for more details.

4.1.10. General procedure J. Oxidation of macrocyclic alcohols

Corresponding macrocycle alcohol (0.36 mmol) was suspended in dry DCM (40 mL) under N_2 atmosphere and was added Dess–martin periodinane (1.08 mmol). Reaction mixture was stirred for 4 h at room temperature and quenched with saturated sodium bicarbonate solution containing 10% Sodium thiosulfate (10 mL). Organic layer was separated and aqueous layer was extracted with DCM (2 × 60 mL), combined organic layers were washed with brine (40 mL), dried over anhydrous sodium sulfate and solvent was evaporated on rotary evaporator. See individual experiments for more details.

4.1.11. Methyl ((S)-2-((tert-butoxycarbonyl)amino)pent-4-ynoyl)-L-leucinate ***13a***

Boc-L-Propargylglycine (6.39 g; 30 mmol) in dry DMF (70 mL) was reacted with L-Leu-OMe(HCl) (30 mmol) according to general procedure **A** and crude product was purified using flash chromatography (silica gel; hexane/ethyl acetate 75:25) to give **13a** as a white solid (9.0 g; 89% yield); M.p. 76–78 °C; ^{1}H NMR (400 MHz, DMSO-d_6): δ ppm 0.75–0.97 (m, 6 H), 1.38 (s, 9 H), 1.44–1.74 (m, 3 H), 2.43 (dd, J = 8.70, 2.29 Hz, 1 H), 2.51–2.57 (m, 1 H), 2.82 (br s, 1 H), 3.52–3.71 (m, 3 H), 4.12 (d, J = 5.19 Hz, 1 H), 4.29 (td, J = 4.96, 2.90 Hz, 1 H), 6.97 (d, J = 8.24 Hz, 1 H), 8.24 (d, J = 7.63 Hz, 1 H); HRMS (ESI, m/z) calcd for $C_{17}H_{29}N_2O_5$ $[M+H]^+$ 341.2076. found: 341.2069.

Compounds **13b** and **13c** were prepared using a similar procedure as the one described above.

4.1.12. Methyl (S)-2-((S)-2-((tert-butoxycarbonyl)amino)pent-4-ynamido)-3-cyclohexylpropanoate ***13b***

White solid (9.2 g; 81% yield); M.p 85–87 °C; ^{1}H NMR (400 MHz, DMSO-d_6): δ ppm 0.71–0.99 (m, 2 H), 1.02–1.25 (m, 3 H), 1.29–1.44 (m, 9 H), 1.45–1.76 (m, 8 H), 2.43 (dd, J = 8.79, 2.15 Hz, 1 H), 2.48 (dd, J = 5.08, 2.73 Hz, 1 H), 2.83 (br. s., 1 H), 3.60 (s, 3 H), 4.11 (d, J = 5.47 Hz, 1 H), 4.32 (d, J = 5.08 Hz, 1 H), 6.97 (d, J = 8.20 Hz, 1 H), 8.24 (d, J = 7.42 Hz, 1 H). HRMS (ESI, m/z) calcd for $C_{20}H_{33}N_2O_5$ $[M+H]^+$ 381.2389. found: 381.2382.

4.1.13. Methyl ((S)-2-((tert-butoxycarbonyl)amino)pent-4-ynoyl)-L-phenylalaninate ***13c***

White solid (8.3 g; 74% yield); M.p 81–83 °C; ^{1}H NMR (400 MHz, DMSO-d_6): δ ppm 1.38 (s, 9 H), 2.37 (dd, J = 8.85, 2.14 Hz, 1 H), 2.45 (dd, J = 4.43, 2.59 Hz, 1 H), 2.82 (br s, 1 H), 2.89–2.98 (m, 1 H), 2.99–3.12 (m, 1 H), 3.58 (s, 3 H), 4.06–4.21 (m, 1 H), 4.37–4.57 (m, 1 H), 6.90 (d, J = 8.85 Hz, 1 H), 7.17–7.24 (m, 3 H), 7.25–7.33 (m, 2 H), 8.31 (d, J = 7.63 Hz, 1 H). HRMS (ESI, m/z) calcd for $C_{20}H_{27}N_2O_5$ $[M+H]^+$ 375.1920. found: 375.1909.

4.1.14. Methyl ((S)-2-(((benzyloxy)carbonyl)amino)pent-4-ynoyl)-L-leucinate ***14a***

Compound **13a** (6.8 g; 20 mmol) in dry CH_2Cl_2 (30 mL) was treated with 1 M HCl in dioxane to remove Boc protection according to general procedure **C** and solvent was removed after the reaction, under high vacuum to dryness. To a solution of resulting HCl salt of the amine in dry THF (70 mL) was added DIEA (12.9 g; 100 mmol) and stirred for 30 min. After that, benzyl chloroformate (3.75 g; 22 mmol) was added and the resulting solution was further reacted for 16 h at room temperature. The solvent was removed on the rotary evaporator and the residue was taken up in ethyl acetate (150 mL) and washed sequentially with saturated $NaHCO_3$ (50 mL), 5% HCl (2 × 50 mL) and brine (50 mL). The organic layer was dried over anhydrous sodium sulfate, filtered and solvent was removed on the rotary evaporator to give **14a** as a white solid (6.7 g: 90% yield); M.p 79–80 °C. ^{1}H NMR (400 MHz, DMSO-d_6): δ ppm 0.79–0.93 (m, 6 H), 1.40–1.72 (m, 3 H), 2.36–2.47 (m, 1 H), 2.52–2.60 (m, 1 H), 2.84 (s, 1 H), 3.55–3.66 (m, 3 H), 4.15–4.32 (m, 2 H), 4.98–5.12 (m, 2 H), 7.24–7.42 (m, 5 H), 7.54 (d, J = 8.54 Hz, 1 H), 8.36 (d, J = 7.63 Hz, 1 H). HRMS (ESI, m/z) calcd for $C_{20}H_{27}N_2O_5$ $[M+H]^+$ 375.1920. found: 375.1916.

Compounds **14b** and **14c** were prepared according to the same procedure as above.

4.1.15. Methyl (S)-2-((S)-2-(((benzyloxy)carbonyl)amino)pent-4-ynamido)-3-cyclohexylpropanoate ***14b***

White solid (7.6 g: 92% yield); M.p 86–88 °C. ^{1}H NMR (400 MHz, DMSO-d_6): δ ppm 0.70–0.99 (m, 2 H), 1.02–1.24 (m, 3 H), 1.33 (br. s., 1 H), 1.43–1.56 (m, 2 H), 1.62 (d, J = 12.21 Hz, 5 H), 2.37–2.48 (m, 1 H), 2.85 (s, 1 H), 3.60 (s, 3 H), 4.22 (td, J = 8.85, 4.88 Hz, 1 H), 4.27–4.35 (m, 1 H), 5.04 (s, 2 H), 7.34–7.41 (m, 5 H), 7.54 (d, J = 8.54 Hz, 1 H), 8.35 (d, J = 7.63 Hz, 1 H). HRMS (ESI, m/z) calcd for $C_{23}H_{31}N_2O_5$ $[M+H]^+$ 415.2233. found: 415.2228.

4.1.16. Methyl ((S)-2-(((benzyloxy)carbonyl)amino)pent-4-ynoyl)-L-phenylalaninate ***14c***

White solid (6.9 g: 85% yield); M.p 106–108 °C. ^{1}H NMR (400 MHz, DMSO-d_6): δ ppm 2.31–2.44 (m, 1 H), 2.54 (dd, J = 4.49, 2.54 Hz, 1 H), 2.84 (s, 1 H), 2.89–2.98 (m, 1 H), 2.99–3.08 (m, 1 H), 3.52–3.63 (m, 3 H), 4.23 (td, J = 8.98, 4.69 Hz, 1 H), 4.41–4.54 (m, 1 H), 4.99–5.10 (m, 2 H), 7.15–7.23 (m, 3 H), 7.24–7.29 (m, 2 H), 7.30–7.42 (m, 5 H), 7.50 (d, J = 8.98 Hz, 1 H), 8.44 (d, J = 7.42 Hz, 1 H). HRMS (ESI, m/z) calcd for $C_{23}H_{25}N_2O_5$ $[M+H]^+$ 409.1763. found: 409.1754.

4.1.17. ((S)-2-(((benzyloxy)carbonyl)amino)pent-4-ynoyl)-L-leucine ***15a***

A solution of compound **14a** (5.6 g; 15 mmol) in dry THF (60 mL) was hydrolyzed according to general procedure B. The crude product was purified by Flash chromatography (Silica gel; Hexane/Ethyl acetate 50:50) to give **15a** as a colorless oil (4.5 g; 84% yield); ^{1}H NMR (400 MHz, DMSO-d_6): δ 0.80–0.95 (m, 6 H), 1.44–1.57 (m, 2 H), 1.59–1.70 (m, 1 H), 1.72–1.81 (m, 2 H), 2.35–2.48 (m, 1 H), 2.52–2.66 (m, 1 H), 2.79–2.86 (m, 1 H), 3.52–3.68 (m, 2 H), 4.11–4.32 (m, 2 H), 5.04 (s, 2 H), 7.25–7.43 (m, 6 H), 7.54 (d, J = 8.59 Hz, 1 H), 8.18 (d, J = 8.20 Hz, 1 H), 12.58 (br. s., 1 H). HRMS (ESI, m/z) calcd for $C_{19}H_{25}N_2O_5$ $[M+H]^+$ 361.1763. found: 361.1758.

Compounds **15b** and **15c** were prepared using the same procedure as described above.

4.1.18. (S)-2-((S)-2-(((benzyloxy)carbonyl)amino)pent-4-ynamido)-3-cyclohexylpropanoic acid ***15b***

Colorless oil (5.2 g; 88% yield); ^{1}H NMR (400 MHz, DMSO-d_6): δ 0.69–0.98 (m, 2 H), 1.05–1.21 (m, 3 H), 1.27–1.41 (m, 1 H), 1.53 (t, J = 7.17 Hz, 2 H), 1.56–1.73 (m, 5 H), 2.36–2.48 (m, 1 H), 2.52–2.62 (m, 1 H), 2.82 (s, 1 H), 4.16–4.32 (m, 2 H), 5.05 (s, 2 H), 7.27–7.43 (m, 5 H), 7.55 (d, J = 8.85 Hz, 1 H), 8.18 (d, J = 7.93 Hz, 1 H), 12.50 (br. s., 1 H). HRMS (ESI, m/z) calcd for $C_{22}H_{29}N_2O_5$ $[M+H]^+$ 401.2076. found: 401.2068.

*4.1.19. ((S)-2-(((benzyloxy)carbonyl)amino)pent-4-ynoyl)-L-phenylalanine **15c***

Colorless oil (5.1 g; 86% yield); ^{1}H NMR (400 MHz, DMSO-d$_6$): δ 2.32–2.44 (m, 1 H), 2.51–2.59 (m, 1 H), 2.82 (s, 1 H), 2.86–2.97 (m, 1 H), 3.00–3.11 (m, 1 H), 4.23 (td, J = 9.18, 4.30 Hz, 1 H), 4.42 (td, J = 8.10, 5.27 Hz, 1 H), 5.01–5.07 (m, 2 H), 7.15–7.29 (m, 5 H), 7.30–7.42 (m, 5 H), 7.52 (d, J = 8.59 Hz, 1 H), 8.21 (d, J = 7.81 Hz, 1 H), 12.69 (br. s., 1 H). HRMS (ESI, m/z) calcd for $C_{22}H_{23}N_2O_5$ $[M+H]^+$ 395.1607. found: 395.1599.

*4.1.20. Methyl N5-(3-azidoropyl)-N2-(tert-butyoxycarbonyl)-L-glutaminate **19a***

A solution of 2-(Boc-amino)-1-ethanol (9.6 g: 60 mmol) in dry DCM (100 mL) was converted in to mesylate according to general procedure **D** to yield **16b** as a colorless oil (13.4 g; 94% yield).

Compound **16a** (11.9 g; 50 mmol) was dissolve in dry DMF (120 mL) and converted in to azide according to general procedure **E** to yield **17a** as a light yellow oil (7.2 g; 78% yield).

A solution of compound **17a** (6.8 g; 37 mmol) in dry CH_2Cl_2 (30 mL) was treated with 1 M HCl in dioxane to remove Boc protection according to general procedure **C** and solvent was removed after the reaction under high vacuum to dryness resulting compound **18a**.

Boc–Glu–OMe (9.67 g; 37 mmol) in dry DMF (100 mL) was reacted with compound **18a** (4.5 g: 37 mmol) according to general procedure **A** and the crude product was purified by flash chromatography (silica gel; hexane/ethyl acetate 70:30) to give **19a** as a colorless oil (9.5 g; 78% yield); ^{1}H NMR (400 MHz, DMSO-d6): δ 1.27–1.47 (m, 9 H), 1.68–1.83 (m, 1 H), 1.86–1.97 (m, 1 H), 2.16 (t, J = 7.42 Hz, 2 H), 3.23 (q, J = 5.60 Hz, 2 H), 3.30–3.40 (m, 2 H), 3.62 (s, 3 H), 3.96 (d, J = 4.69 Hz, 1 H), 7.24 (d, J = 7.42 Hz, 1 H), 8.06 (br. s., 1 H). HRMS (ESI, m/z) calcd for $C_{13}H_{24}N_5O_5$ $[M+H]^+$ 330.1777. found: 330.1769.

Compounds **19b**–**e** were prepared using the same procedure as described above.

*4.1.21. Methyl N^5-(3-azidopropyl)-N^2-(tert-butoxycarbonyl)-L-glutaminate **19b***

Colorless oil (8.2 g; 72% yield); ^{1}H NMR (400 MHz, DMSO-d$_6$): δ 1.27–1.44 (m, 9 H), 1.63 (q, J = 6.84 Hz, 2 H), 1.69–1.81 (m, 1 H), 1.85–1.98 (m, 1 H), 2.14 (t, J = 7.42 Hz, 2 H), 3.01–3.18 (m, 2 H), 3.28–3.41 (m, 2 H), 3.62 (s, 3 H), 3.94 (dd, J = 8.01, 3.32 Hz, 1 H), 7.23 (d, J = 7.81 Hz, 1 H), 7.87 (d, J = 4.69 Hz, 1 H). HRMS (ESI, m/z) calcd for $C_{14}H_{26}N_5O_5$ $[M+H]^+$ 344.1934. found: 344.1929.

*4.1.22. Methyl N^5-(4-azidobutyl)-N^2-(tert-butoxycarbonyl)-L-glutaminate **19c***

Colorless oil (9.0 g: 85% yield); ^{1}H NMR (400 MHz, DMSO-d$_6$): δ 1.29–1.40 (m, 9 H), 1.40–1.58 (m, 4 H), 1.66–1.80 (m, 1 H), 1.84–1.97 (m, 1 H), 2.13 (t, J = 7.42 Hz, 2 H), 3.04 (q, J = 6.25 Hz, 2 H), 3.32 (t, J = 6.84 Hz, 2 H), 3.62 (s, 3 H), 3.94 (dd, J = 8.01, 3.71 Hz, 1 H), 7.23 (d, J = 7.81 Hz, 1 H), 7.71–7.91 (m, 1 H). HRMS (ESI, m/z) calcd for $C_{15}H_{28}N_5O_5$ $[M+H]^+$ 358.2090. found: 358.2083.

*4.1.23. Methyl N^5-(5-azidopentyl)-N^2-(tert-butoxycarbonyl)-L-glutaminate **19d***

Colorless oil (7.9 g: 69% yield); ^{1}H NMR (400 MHz, DMSO-d$_6$): δ 1.24–1.34 (m, 3 H), 1.35–1.44 (m, 10 H), 1.52 (q, J = 7.13 Hz, 2 H), 1.66–1.81 (m, 1 H), 1.84–1.97 (m, 1 H), 2.13 (t, J = 7.42 Hz, 2 H), 3.02 (q, J = 6.12 Hz, 2 H), 3.26–3.37 (m, 2 H), 3.62 (s, 3 H), 3.94 (d, J = 4.30 Hz, 1 H), 7.23 (d, J = 7.81 Hz, 1 H), 7.78 (t, J = 5.27 Hz, 1 H). HRMS (ESI, m/z) calcd for $C_{16}H_{30}N_5O_5$ $[M+H]^+$ 372.2247. found: 372.2241.

*4.1.24. Methyl N^5-(6-azidohexyl)-N^2-(tert-butoxycarbonyl)-L-glutaminate **19e***

Yellow oil (6.5 g: 68% yield); ^{1}H NMR (400 MHz, DMSO-d$_6$): δ 1.24–1.30 (m, 3 H), 1.31–1.35 (m, 3 H), 1.36–1.41 (m, 9 H), 1.44–1.60 (m, 2 H), 1.73 (br. s., 1 H), 1.86–1.96 (m, 1 H), 2.12 (t, J = 7.48 Hz, 2 H), 3.01 (q, J = 6.21 Hz, 2 H), 3.22–3.36 (m, 2 H), 3.62 (s, 3 H), 3.94 (d, J = 4.27 Hz, 1 H), 7.23 (d, J = 7.63 Hz, 1 H), 7.76 (d, J = 5.19 Hz, 1 H). HRMS (ESI, m/z) calcd for $C_{17}H_{32}N_5O_5$ $[M+H]^+$ 386.2403. found: 386.2401.

*4.1.25. Methyl N^5-(3-azidopropyl)-L-glutaminate hydrochloride **20a***

A solution of compound **19a** (4.4 g: 15 mmol) in dry DCM (20 mL) was treated with 4 M HCl in dioxane according to general procedure C to obtain compound **20a** as a yellow oil (4.0 g; 95% yield); ^{1}H NMR (400 MHz, DMSO-d$_6$): δ 1.63 (q, J = 6.88 Hz, 2 H), 1.67–1.80 (m, 1 H), 1.85–1.98 (m, 1 H), 2.14 (t, J = 7.42 Hz, 2 H), 3.01–3.18 (m, 2 H), 3.28–3.41 (m, 2 H), 3.62 (s, 3 H), 3.94 (dd, J = 8.01, 3.32 Hz, 1 H), 7.23 (d, J = 7.81 Hz, 1 H), 7.87 (d, J = 4.69 Hz, 1 H). HRMS (ESI, m/z) calcd for $C_9H_{19}ClN_5O_3$ $[M+H]^+$ 280.1176. found: 280.1172.

Compound **20b** was prepared using the same procedure as described above.

*4.1.26. Methyl N^5-(4-azidobutyl)-L-glutaminate hydrochloride **20b***

Yellow oil (4.8 g; 94% yield); ^{1}H NMR (400 MHz, DMSO-d$_6$): δ 1.39–1.57 (m, 4 H), 1.66–1.80 (m, 1 H), 1.84–1.97 (m, 1 H), 2.13 (t, J = 7.42 Hz, 2 H), 3.04 (q, J = 6.25 Hz, 2 H), 3.33 (t, J = 6.84 Hz, 2 H), 3.62 (s, 3 H), 3.94 (dd, J = 8.01, 3.71 Hz, 1 H), 7.23 (d, J = 7.81 Hz, 1 H), 7.71–7.91 (m, 1 H). HRMS (ESI, m/z) calcd for $C_{10}H_{21}ClN_5O_3$ $[M+H]^+$ 294.1333. found: 294.1330.

*4.1.27. 5-Azido-2-(((benzyloxy)carbonyl)amino)pentanoic acid **21** [35]*

To a solution of sodium azide (2.27 g; 35 mmol) suspended in anhydrous acetonitrile (35 mL) at 0 °C was added triflic anhydride (8.18 g; 29 mmol) dropwise over 10 min and the cooled solution was stirred for 2 h. The mixture was filtered through cotton wool to give a crude triflic azide solution. To a vigorously stirred suspension of Z-L-ornithine (6.39 g; 24 mmol) in acetonitrile (100 mL) and water (40 mL) mixture was added trimethylamine (7.38 g; 73 mmol) and $CuSO_4$ (24 mmol). The resulting solution was cooled to ^{0}C and the triflic azide solution was added dropwise. After 30 min, cooling was removed and the reaction mixture was stirred at room temperature overnight. The solvent was removed on the rotary evaporator and the aqueous solution was washed with ethyl acetate (2 × 100 mL). The aqueous phase was then acidified with 2 M HCl followed by concentrated HCl and extracted with ethyl acetate (3 × 100 mL). The organic layer was dried over anhydrous sodium sulfate, filtered, and concentrated to yield a crude product. After that chloroform was added and the solution was refrigerated and the precipitate was filtered off. The solvent was removed on the rotary evaporator and the crude product was purified using flash chromatography to obtain compound **21** as a light yellow oil (2.14 g; 30% yield); ^{1}H NMR (400 MHz, DMSO-d$_6$): δ 1.45–1.71 (m, 3 H), 1.72–1.87 (m, 1 H), 3.32 (t, J = 6.41 Hz, 2 H), 3.96–4.02 (m, 1 H), 5.05 (s, 2 H), 7.23–7.46 (m, 5 H), 7.62 (d, J = 7.93 Hz, 1 H), 12.10 (b. s., 1H). HRMS (ESI, m/z) calcd for $C_{13}H_{17}N_4O_4$ $[M+H]^+$ 293.1250. found: 293.1248.

*4.1.28. Methyl N^2-(tert-butoxycarbonyl)-N^5-(prop-2-yn-1-yl)-L-glutaminate **22***

To a solution of Boc–Glu–OMe (5.2 g; 20 mmol) in dry DMF (60 mL) was added EDCI (4.67 g; 24.4 mmol), HOBt (3.7 g; 24.4 mmol) and the reaction mixture was stirred at room

temperature for 30 min. Propargylamine (1.1 g; 20 mmol) was added to the mixture and the reaction mixture was stirred overnight at room temperature. The solvent was removed on the rotary evaporator and residue was taken up with DCM (400 mL) and washed sequentially with 10% aqueous citric acid (150 mL) and brine (150 mL). The organic layer was dried over anhydrous sodium sulfate, filtered, and concentrated to yield a crude product which was purified by flash chromatography (silica gel; hexane/ethyl acetate 50:50) to give **22** as a colorless oil (3.8 g; 64% yield); ^{1}H NMR (400 MHz, DMSO-d_6): δ ppm 1.35 (s, 9 H), 1.96–2.10 (m, 2 H), 2.19–2.30 (m, 1 H), 2.30–2.42 (m, 1 H), 3.12 (t, J = 2.29 Hz, 1 H), 3.69–3.78 (m, 3 H), 3.85 (dd, J = 5.34, 2.44 Hz, 2 H), 3.96–4.08 (m, 1 H), 7.81 (d, J = 6.81 Hz, 1H), 8.48 (t, J = 5.19 Hz, 1 H). HRMS (ESI, m/z) calcd for $C_{14}H_{23}N_2O_5$ $[M+H]^+$ 299.1607. found: 299.1602.

*4.1.29. Methyl N^2-((tert-butoxycarbonyl)leucyl)-N^5-(prop-2-yn-1-yl)-L-glutaminate **23***

A solution of compound **22** (8.91 g; 30 mmol) in dry DCM (90 mL) was treated with 1 M HCl in dioxane according to general procedure **C**. The resulting compound was coupled with Boc–Glu–OMe (7.74 g; 30 mmol) in dry DMF (70 mL) according to general procedure **A** and the crude product was purified by flash chromatography (silica gel; hexane/ethyl acetate 50:50) to give **19a** as a yellow oil (8.0 g; 65% yield); ^{1}H NMR (400 MHz, $CDCl_3$): δ 0.95 (t, J = 6.56 Hz, 6 H), 1.38–1.56 (m, 10 H), 1.65 (dd, J = 13.58, 5.19 Hz, 2 H), 1.85–2.03 (m, 1 H), 2.18–2.39 (m, 4 H), 3.74 (s, 3 H), 4.04 (td, J = 5.04, 2.59 Hz, 2 H), 4.08–4.20 (m, 1 H), 4.54 (br. s., 1 H), 5.02 (d, J = 7.63 Hz, 1 H), 6.80–6.92 (m, 1 H), 6.94–7.07 (m, 1 H). HRMS (ESI, m/z) calcd for $C_{20}H_{34}N_3O_6$ $[M+H]^+$ 412.2448. found: 412.2445.

*4.1.30. Methyl N^5-(3-azidopropyl)-N^2-(((S)-2-(((benzyloxy)carbonyl)amino)pent-4-ynoyl)-L-leucyl)-L-glutaminate **24a***

A solution of compound **15a** (11.7 g; 31 mmol) in dry DMF (100 mL) was coupled with compound **20a** according to general procedure A and the crude product was purified using flash chromatography (silica gel; DCM/methanol 95:5) to obtain compound **24a** as a white solid (8.3 g; 46% yield); M.p 110–111 °C. ^{1}H NMR (400 MHz, DMSO-d_6): δ 0.86 (dd, J = 15.43, 6.44 Hz, 6 H), 1.45 (t, J = 6.84 Hz, 2 H), 1.63 (t, J = 6.64 Hz, 3 H), 1.73–1.87 (m, 1 H), 1.89–2.02 (m, 2 H), 2.07–2.21 (m, 2 H), 2.35–2.48 (m, 2 H), 2.52–2.63 (m, 1 H), 2.82 (br. s., 1 H), 3.01–3.15 (m, 2 H), 3.60 (s, 3 H), 4.11–4.25 (m, 2 H), 4.31 (d, J = 7.03 Hz, 1 H), 5.05 (s, 2 H), 7.23–7.41 (m, 5 H), 7.59 (d, J = 7.81 Hz, 1 H), 7.82 (br. s., 1 H), 7.99 (d, J = 7.78 Hz, 1 H), 8.29 (d, J = 7.42 Hz, 1 H). HRMS (ESI, m/z) calcd for $C_{28}H_{40}N_7O_7$ $[M+H]^+$ 586.2989. found: 586.2986.

Compound **24b** was prepared using the same procedure as described above.

*4.1.31. Methyl N^5-(4-azidobutyl)-N^2-(((S)-2-(((benzyloxy)carbonyl)amino)pent-4-ynoyl)-L-leucyl)-L-glutaminate **24b***

White solid (9.6 g; 58% yield); M.p 106–108 °C. ^{1}H NMR (400 MHz, DMSO-d_6): δ 0.75–0.94 (m, 6 H), 1.34–1.53 (m, 6 H), 1.54–1.69 (m, 2 H), 1.72–1.87 (m, 2 H), 1.94 (dd, J = 13.19, 5.49 Hz, 2 H), 2.04–2.21 (m, 2 H), 2.77–2.90 (m, 1 H), 3.04 (q, J = 6.29 Hz, 2 H), 3.54–3.67 (m, 3 H), 4.10–4.25 (m, 2 H), 4.26–4.39 (m, 2 H), 5.01–5.08 (m, 2 H), 7.28–7.44 (m, 5 H), 7.61 (d, J = 8.42 Hz, 1 H), 7.81 (t, J = 5.40 Hz, 1 H), 8.01 (d, J = 8.24 Hz, 1 H), 8.31 (d, J = 7.14 Hz, 1 H). HRMS (ESI, m/z) calcd for $C_{29}H_{42}N_7O_7$ $[M+H]^+$ 600.3146. found: 600.3144.

*4.1.32. Methyl (3S,6S,9S,Z)-3-(((benzyloxy)carbonyl)amino)-6-isobutyl-4,7,12-trioxo-1^{1}H-5,8,13-triaza-1(4,1)-triazolacyclohexadecaphane-9-carboxylate **25a***

A solution of compound **24a** (0.3 g: 0.512 mmol) in dry DCM (420 mL) was cyclized according to general procedure **G** and the crude product was purified using flash chromatography (silica gel; DCM/methanol 95:5) to give compound **25a** as a white solid (0.14 g; 45% yield); M.p 210–211 °C. ^{1}H NMR (DMSO-d_6): δ 0.73–0.99 (m, 6 H), 1.45 (q, J = 6.60 Hz, 3 H), 1.62–1.80 (m, 2 H), 1.83–1.94 (m, 1 H), 2.00–2.30 (m, 4 H), 2.60–2.76 (m, 1 H), 3.04 (d, J = 4.30 Hz, 2 H), 3.57–3.68 (m, 3 H), 4.08–4.20 (m, 1 H), 4.26–4.45 (m, 4 H), 5.04 (d, J = 9.76 Hz, 2 H), 7.03 (d, J = 7.03 Hz, 1 H), 7.24–7.42 (m, 5 H), 7.53 (s, 2 H), 8.16 (d, J = 7.42 Hz, 1 H), 8.53 (d, J = 8.20 Hz, 1 H). HRMS (ESI, m/z) calcd for $C_{28}H_{40}N_7O_7$ $[M+H]^+$ 586.2989. found: 586.2984.

Compound **25b** was prepared using the same procedure as described above.

*4.1.33. Methyl (3S,6S,9S,Z)-3-(((benzyloxy)carbonyl)amino)-6-isobutyl-4,7,12-trioxo-1^{1}H-5,8,13-triaza-1(4,1)-triazolacycloheptadecaphane-9-carboxylate **25b***

White solid (0.15 g; 50% yield); M.p 213–215 °C. ^{1}H NMR (400 MHz, DMSO-d_6): δ 0.87 (dd, J = 12.69, 6.44 Hz, 6 H), 1.14–1.32 (m, 2 H), 1.35–1.56 (m, 3 H), 1.57–1.83 (m, 4 H), 2.03–2.32 (m, 3 H), 2.73 (t, J = 6.25 Hz, 1 H), 2.98–3.14 (m, 2 H), 3.54–3.70 (m, 3 H), 4.11–4.32 (m, 3 H), 4.32–4.44 (m, 2 H), 4.92–5.16 (m, 2 H), 6.91 (d, J = 7.81 Hz, 1 H), 7.26–7.41 (m, 5 H), 7.67–7.83 (m, 2 H), 8.22 (d, J = 7.42 Hz, 1 H), 8.36 (d, J = 7.81 Hz, 1 H). HRMS (ESI, m/z) calcd for $C_{29}H_{42}N_7O_7$ $[M+H]^+$ 600.3146. found: 600.3142.

*4.1.34. ((S)-2-(((benzyloxy)carbonyl)amino)-3-(1-(2-((S)-4-((tert-butoxycarbonyl)amino)-5-methoxy-5-oxopentanamido)ethyl)-1H-1,2,3-triazol-4-yl)propanoyl)-L-leucine **27a***

Compound **15a** (2.04 g; 5 mmol) was reacted with compound **19a** (1.92 g; 5 mmol) according to general procedure F and the crude product was purified using flash chromatography (silica gel; DCM/methanol 95:5) to give compound **27a** as a white solid (3.17 g; 80% yield); M.p 48–49 °C. ^{1}H NMR (400 MHz, DMSO-d_6): δ 0.68–0.94 (m, 6 H), 1.25–1.41 (m, 9 H), 1.42–1.81 (m, 4 H), 1.84–2.01 (m, 1 H), 2.13 (t, J = 7.23 Hz, 1 H), 2.76–3.12 (m, 2 H), 3.56–3.68 (m, 3 H), 3.94 (d, J = 5.08 Hz, 1 H), 4.15–4.26 (m, 1 H), 4.27–4.42 (m, 3 H), 4.89–5.07 (m, 2 H), 7.24 (d, J = 7.81 Hz, 1 H), 7.28–7.40 (m, 7 H), 7.47 (d, J = 8.20 Hz, 1 H), 7.69–7.80 (m, 1 H), 7.91–8.03 (m, 1 H), 8.24 (d, J = 7.81 Hz, 1 H). HRMS (ESI, m/z) calcd for $C_{32}H_{48}N_7O_{10}$ $[M+H]^+$ 690.3463. found: 690.3462.

Compound **27b-27i** was prepared using the same procedure as described above.

*4.1.35. (S)-2-((S)-2-(((benzyloxy)carbonyl)amino)-3-(1-(2-((S)-4-((tert-butoxycarbonyl)amino)-5-methoxy-5-oxopentanamido)ethyl)-1H-1,2,3-triazol-4-yl)propanamido)-3-cyclohexylpropanoic acid **27b***

White solid (3.4 g; 84%); M.p 51–53 °C. ^{1}H NMR (400 MHz, DMSO-d_6): δ 0.67–1.00 (m, 2 H), 1.11 (d, J = 7.42 Hz, 2 H), 1.28–1.45 (m, 10 H), 1.48–1.81 (m, 8 H), 1.83–1.95 (m, 1 H), 2.13 (t, J = 7.23 Hz, 2 H), 2.87 (dd, J = 14.84, 9.37 Hz, 1 H), 3.04 (dd, J = 14.84, 4.69 Hz, 1 H), 3.40–3.52 (m, 3 H), 3.61 (s, 3 H), 3.87–3.98 (m, 1 H), 4.18–4.45 (m, 4 H), 4.86–5.10 (m, 2 H), 7.23 (d, J = 7.81 Hz, 1 H), 7.27–7.39 (m, 5 H), 7.47 (d, J = 8.59 Hz, 1 H), 7.75 (s, 1 H), 7.96 (t, J = 5.27 Hz, 1 H), 8.22 (d, J = 7.81 Hz, 1 H). HRMS (ESI, m/z) calcd for $C_{35}H_{52}N_7O_{10}$ $[M+H]^+$ 730.3776. found: 730.3774.

*4.1.36. (S)-2-((S)-2-(((benzyloxy)carbonyl)amino)-3-(1-(3-((S)-4-((tert-butoxycarbonyl)amino)-5-methoxy-5-oxopentanamido)propyl)-1H-1,2,3-triazol-4-yl)propanamido)-3-cyclohexylpropanoic acid **27c***

White solid (3.2 g; 82% yield); M.p 52–53 °C. ^{1}H NMR (400 MHz, DMSO-d_6): δ 0.68–0.99 (m, 2 H), 1.12 (d, J = 6.25 Hz, 2 H), 1.24–1.44 (m, 10 H), 1.45–1.82 (m, 8 H), 1.83–1.97 (m, 3 H), 2.06–2.27 (m, 2 H), 2.77–2.94 (m, 1 H), 2.95–3.15 (m, 3 H), 3.62 (s, 3 H), 3.88–3.99 (m, 1 H), 4.16–4.40 (m, 4 H), 4.89–5.07 (m, 2 H), 7.25 (d, J = 7.42 Hz,

1 H), 7.29–7.41 (m, 5 H), 7.49 (d, $J = 8.59$ Hz, 1 H), 7.78 (s, 1 H), 7.92 (d, $J = 4.69$ Hz, 1 H), 8.24 (d, $J = 7.42$ Hz, 1 H). HRMS (ESI, *m*/*z*) calcd for $C_{36}H_{54}N_7O_{10}$ $[M+H]^+$ 744.3932. found: 744.3929.

4.1.37. (S)-2-((S)-2-(((benzyloxy)carbonyl)amino)-3-(1-(4-((S)-4-((tert-butoxycarbonyl)amino)-5-methoxy-5-oxopentanamido) butyl)-1H-1,2,3-triazol-4-yl)propanamido)-3-cyclohexylpropanoic acid ***27d***

White solid (3.3 g; 82% yield); M.p 58–60 °C. ^{1}H NMR (400 MHz, DMSO-d_6): δ 0.64–0.10 (m, 2 H), 1.11–1.18 (m, 3 H), 1.22–1.43 (m, 10 H), 1.45–1.82 (m, 8 H), 1.83–1.99 (m, 3 H), 2.06–2.29 (m, 3 H), 2.78–2.94 (m, 1 H), 2.95–3.17 (m, 3 H), 3.64 (s, 3 H), 3.88–4.00 (m, 1 H), 4.15–4.40 (m, 4 H), 4.89–5.05 (m, 2 H), 7.28 (d, $J = 7.47$ Hz, 1 H), 7.30–7.41 (m, 5 H), 7.50 (d, $J = 8.78$ Hz, 1 H), 7.77 (s, 1 H), 7.92 (d, $J = 4.46$ Hz, 1 H), 8.27 (d, $J = 7.50$ Hz, 1 H). HRMS (ESI, *m*/*z*) calcd for $C_{37}H_{56}N_7O_{10}$ $[M+H]^+$ 758.4089. found: 758.4087.

4.1.38. ((S)-2-(((benzyloxy)carbonyl)amino)-3-(1-(5-((S)-4-((tert-butoxycarbonyl)amino)-5-methoxy-5-oxopentanamido)pentyl)-1H-1,2,3-triazol-4-yl)propanoyl)-L-leucine ***27e***

White solid (3.6 g; 87% yield); M.p 56–58 °C. ^{1}H NMR (400 MHz, DMSO-d_6): δ 0.69–0.99 (m, 6 H), 1.10–1.25 (m, 3 H), 1.28–1.44 (m, 12 H), 1.47–1.81 (m, 5 H), 1.84–1.98 (m, 1 H), 2.12 (t, $J = 7.23$ Hz, 2 H), 2.74–2.92 (m, 1 H), 2.99 (d, $J = 5.86$ Hz, 3 H), 3.62 (s, 3 H), 3.94 (d, $J = 4.69$ Hz, 1 H), 4.27 (br. s., 4 H), 4.99 (d, $J = 4.30$ Hz, 2 H), 7.26 (d, $J = 7.42$ Hz, 1 H), 7.30–7.41 (m, 5 H), 7.49 (d, $J = 8.20$ Hz, 1 H), 7.68–7.87 (m, 2 H), 8.08–8.49 (m, 1 H). HRMS (ESI, *m*/*z*) calcd for $C_{35}H_{54}N_7O_{10}$ $[M+H]^+$ 732.3932. found: 732.3930.

4.1.39. (S)-2-((S)-2-(((benzyloxy)carbonyl)amino)-3-(1-(5-((S)-4-((tert-butoxycarbonyl)amino)-5-methoxy-5-oxopentanamido) pentyl)-1H-1,2,3-triazol-4-yl)propanamido)-3-cyclohexylpropanoic acid ***27f***

White solid (3.5 g; 82% yield); M.p 55–57 °C. ^{1}H NMR (400 MHz, DMSO-d_6): δ 0.71–0.99 (m, 2 H), 1.01–1.25 (m, 5 H), 1.26–1.45 (m, 12 H), 1.46–1.82 (m, 10 H), 1.82–1.97 (m, 1 H), 2.12 (t, $J = 7.23$ Hz, 2 H), 2.84 (br. s., 1 H), 2.94–3.11 (m, 3 H), 3.62 (s, 3 H), 3.94 (d, $J = 4.69$ Hz, 1 H), 4.27 (br. s., 4 H), 4.89–5.08 (m, 2 H), 7.20–7.41 (m, 6 H), 7.50 (d, $J = 8.20$ Hz, 1 H), 7.77 (d, $J = 14.45$ Hz, 2 H), 8.13–8.41 (m, 1 H). HRMS (ESI, *m*/*z*) calcd for $C_{38}H_{58}N_7O_{10}$ $[M+H]^+$ 772.4245. found: 772.4243.

4.1.40. ((S)-2-(((benzyloxy)carbonyl)amino)-3-(1-(6-((S)-4-((tert-butoxycarbonyl)amino)-5-methoxy-5-oxopentanamido)hexyl)-1H-1,2,3-triazol-4-yl)propanoyl)-L-leucine ***27g***

White solid (3.9 g; 88% yield); M.p 59–61 °C. ^{1}H NMR (400 MHz, DMSO-d_6): δ 0.72–0.94 (m, 6 H), 1.15–1.28 (m, 5 H), 1.29–1.43 (m, 11 H), 1.45–1.81 (m, 5 H), 1.83–1.96 (m, 1 H), 2.12 (t, $J = 7.23$ Hz, 2 H), 2.78–2.92 (m, 1 H), 2.94–3.11 (m, 3 H), 3.61 (s, 3 H), 3.93 (d, $J = 4.69$ Hz, 1 H), 4.27 (br. s., 4 H), 4.86–5.07 (m, 2 H), 7.26 (d, $J = 7.42$ Hz, 1 H), 7.28–7.40 (m, 5 H), 7.48 (d, $J = 8.20$ Hz, 1 H), 7.67–7.87 (m, 2 H), 8.13–8.40 (m, 1 H). HRMS (ESI, *m*/*z*) calcd for $C_{36}H_{56}N_7O_{10}$ $[M+H]^+$ 746.4089. found: 746.4088.

4.1.41. (S)-2-((S)-2-(((benzyloxy)carbonyl)amino)-3-(1-(6-((S)-4-((tert-butoxycarbonyl)amino)-5-methoxy-5-oxopentanamido) hexyl)-1H-1,2,3-triazol-4-yl)propanamido)-3-cyclohexylpropanoic acid ***27h***

White solid (3.3 g; 84% yield); M.p 58–60 °C. ^{1}H NMR (400 MHz, DMSO-d_6): δ 0.65–0.95 (m, 2 H), 1.08 (d, $J = 7.93$ Hz, 2 H), 1.19 (br. s., 4 H), 1.26–1.39 (m, 13 H), 1.44–1.76 (m, 10 H), 1.78–1.93 (m, 1 H), 2.08 (t, $J = 7.17$ Hz, 2 H), 2.73–2.88 (m, 1 H), 2.90–3.06 (m, 3 H), 3.58 (s, 3 H), 3.83–3.95 (m, 1 H), 4.23 (t, $J = 6.71$ Hz, 4 H), 4.95 (d, $J = 3.97$ Hz, 2 H), 7.20 (d, $J = 7.63$ Hz, 1 H), 7.23–7.36 (m, 5 H), 7.40–7.48 (m, 1 H), 7.71 (br. s., 2 H), 8.10–8.32 (m, 1 H). HRMS (ESI, *m*/*z*) calcd for $C_{39}H_{60}N_7O_{10}$ $[M+H]^+$ 786.4402. found: 786.4401.

4.1.42. ((S)-2-(((benzyloxy)carbonyl)amino)-3-(1-(6-((S)-4-((tert-butoxycarbonyl)amino)-5-methoxy-5-oxopentanamido)hexyl)-1H-1,2,3-triazol-4-yl)propanoyl)-L-phenylalanine ***27i***

White solid (3.41 g; 81% yield); M.p 112–116 °C. ^{1}H NMR (400 MHz, DMSO-d_6): δ 1.12–1.44 (m, 14 H), 1.46–1.59 (m, 1 H), 1.64–1.81 (m, 2 H), 1.82–2.00 (m, 1 H), 2.12 (t, $J = 6.44$ Hz, 2 H), 2.82 (br. s., 1 H), 2.89–3.12 (m, 5 H), 3.61 (d, $J = 2.34$ Hz, 3 H), 3.94 (d, $J = 4.69$ Hz, 1 H), 4.26 (t, $J = 6.64$ Hz, 4 H), 4.39–4.53 (m, 1 H), 4.97 (s, 2 H), 7.10–7.40 (m, 11 H), 7.45 (d, $J = 8.20$ Hz, 1 H), 7.69 (br. s., 1 H), 7.76 (d, $J = 4.30$ Hz, 1 H), 8.08–8.41 (m, 1 H). HRMS (ESI, *m*/*z*) calcd for $C_{39}H_{54}N_7O_{10}$ $[M+H]^+$ 780.3932. found: 780.3929.

4.1.43. Methyl (8S,11S,14S,Z)-14-(((benzyloxy)carbonyl)amino)-11-isobutyl-5,10,13-trioxo-1^1*H-4,9,12-triaza-1(1,4)-triazolacyclopentadecaphane-8-carboxylate* ***28a***

A solution of compound **27a** (0.69 g; 1 mmol) in dry CH_2Cl_2 (5 mL) was treated with 1 M HCl in dioxane according to general procedure **C**. The resulting compound was cyclized in dry DMF (500 mL) according to general procedure **H** and the crude product was purified by flash chromatography (silica gel; DCM/methanol 95:5) to give compound **28a** as a white solid (0.34 g; 60% yield); M.p 203–205 °C. ^{1}H NMR (400 MHz, DMSO-d_6): δ 0.77–1.01 (m, 6 H), 1.34–1.59 (m, 3 H), 1.76 (dt, $J = 13.28$, 6.64 Hz, 1 H), 2.12 (d, $J = 16.80$ Hz, 1 H), 2.26 (t, $J = 12.89$ Hz, 1 H), 2.37–2.48 (m, 1 H), 2.75–2.91 (m, 1 H), 3.01–3.11 (m, 1 H), 3.24 (d, $J = 12.89$ Hz, 1 H), 3.59–3.69 (m, 3 H), 3.71–3.83 (m, 1 H), 4.01–4.20 (m, 2 H), 4.37–4.54 (m, 2 H), 4.61–4.74 (m, 1 H), 4.94–5.17 (m, 2 H), 6.60 (d, $J = 8.20$ Hz, 1 H), 7.22–7.43 (m, 6 H), 7.68 (s, 1 H), 8.28 (d, $J = 4.69$ Hz, 1 H), 8.45 (d, $J = 9.76$ Hz, 1 H). HRMS (ESI, *m*/*z*) calcd for $C_{27}H_{38}N_7O_7$ $[M+H]^+$ 572.2833. found: 572.2830.

Compound **28b**–**28i** was prepared using the same procedure as described above.

4.1.44. Methyl (8S,11S,14S,Z)-14-(((benzyloxy)carbonyl)amino)-11-(cyclohexylmethyl)-5,10,13-trioxo-1^1*H-4,9,12-triaza-1(1,4)-triazolacyclopentadecaphane-8-carboxylate* ***28b***

White solid (0.37 g; 62% yield); M.p > 230 °C. ^{1}H NMR (400 MHz, DMSO-d_6): δ 0.79–0.96 (m, 2 H), 1.03–1.30 (m, 3 H), 1.46 (br. s., 4 H), 1.57–1.72 (m, 4 H), 1.75–1.89 (m, 1 H), 2.04–2.16 (m, 1 H), 2.18–2.33 (m, 1 H), 2.37–2.47 (m, 1 H), 2.74–2.91 (m, 1 H), 2.99–3.12 (m, 1 H), 3.15–3.26 (m, 1 H), 3.65 (s, 3 H), 3.71–3.82 (m, 1 H), 4.02–4.18 (m, 2 H), 4.37–4.52 (m, 2 H), 4.60–4.74 (m, 1 H), 5.04 (d, $J = 7.03$ Hz, 2 H), 6.61 (d, $J = 8.60$ Hz, 1 H), 7.22–7.44 (m, 6 H), 7.68 (s, 1 H), 8.25 (d, $J = 4.41$ Hz, 1 H), 8.41 (d, $J = 9.41$ Hz, 1 H). HRMS (ESI, *m*/*z*) calcd for $C_{30}H_{42}N_7O_7$ $[M+H]^+$ 612.3146. found: 612.3144.

4.1.45. Methyl (3S,6S,9S,Z)-3-(((benzyloxy)carbonyl)amino)-6-(cyclohexylmethyl)-4,7,12-trioxo-1^1*H-5,8,13-triaza-1(4,1)-triazolacyclohexadecaphane-9-carboxylate* ***28c***

White solid (0.4 g; 65% yield); M.p > 230 °C. ^{1}H NMR (400 MHz, DMSO-d_6): δ 0.73–0.95 (m, 2 H), 1.02–1.26 (m, 3 H), 1.30–1.53 (m, 3 H), 1.54–1.79 (m, 6 H), 1.83–1.93 (m, 1 H), 1.98–2.29 (m, 4 H), 2.66 (dd, $J = 13.28$, 6.25 Hz, 1 H), 3.03 (d, $J = 5.86$ Hz, 2 H), 3.19–3.30 (m, 1 H), 3.63 (s, 3 H), 4.13 (dt, $J = 13.67$, 6.44 Hz, 1 H), 4.22–4.43 (m, 4 H), 4.94–5.11 (m, 2 H), 7.06 (d, $J = 7.81$ Hz, 1 H), 7.25–7.41 (m, 5 H), 7.46–7.58 (m, 2 H), 8.14 (d, $J = 7.42$ Hz, 1 H), 8.52 (d, $J = 8.20$ Hz, 1 H). HRMS (ESI, *m*/*z*) calcd for $C_{31}H_{44}N_7O_7$ $[M+H]^+$ 626.3302. found: 626.3329.

4.1.46. Methyl (3S,6S,9S,Z)-3-(((benzyloxy)carbonyl)amino)-6-(cyclohexylmethyl)-4,7,12-trioxo-1^1*H-5,8,13-triaza-1(4,1)-triazolacycloheptadecaphane-9-carboxylate* ***28d***

White solid (0.39 g; 62% yield); M.p 206–207 °C. ^{1}H NMR

(400 MHz, DMSO-d_6): δ 0.75–0.99 (m, 2 H), 1.03–1.29 (m, 4 H), 1.44 (d, J = 9.76 Hz, 3 H), 1.50–1.81 (m, 10 H), 2.04–2.31 (m, 3 H), 2.65–2.79 (m, 1 H), 2.95–3.16 (m, 2 H), 3.62 (s, 3 H), 4.10–4.20 (m, 1 H), 4.22–4.31 (m, 2 H), 4.32–4.49 (m, 2 H), 4.93–5.14 (m, 2 H), 7.00 (d, J = 7.42 Hz, 1 H), 7.25–7.47 (m, 5 H), 7.76 (s, 2 H), 8.22 (d, J = 7.42 Hz, 1 H), 8.35 (d, J = 7.81 Hz, 1 H). HRMS (ESI, m/z) calcd for $C_{32}H_{46}N_7O_7$ $[M+H]^+$ 640.3459. found: 640.3457.

4.1.47. Methyl (3S,6S,9S,Z)-3-(((benzyloxy)carbonyl)amino)-6-isobutyl-4,7,12-trioxo-1^{1}H-5,8,13-triaza-1(4,1)-triazolacyclooctadecaphane-9-carboxylate ***28e***

White solid (0.36 g; 59% yield); M.p 209–211 °C. ^{1}H NMR (400 MHz, DMSO-d_6): δ 0.86 (dd, J = 19.53, 6.25 Hz, 6 H), 1.06–1.24 (m, 2 H), 1.28–1.56 (m, 4 H), 1.58–1.82 (m, 3 H), 1.91 (dt, J = 14.06, 7.03 Hz, 1 H), 1.98–2.06 (m, 1 H), 2.07–2.22 (m, 2 H), 2.88–3.16 (m, 4 H), 3.62 (s, 3 H), 4.11 (q, J = 6.77 Hz, 1 H), 4.16–4.25 (m, 1 H), 4.26–4.41 (m, 3 H), 4.92–5.15 (m, 2 H), 7.23 (d, J = 7.42 Hz, 1 H), 7.28–7.43 (m, 5 H), 7.55–7.74 (m, 2 H), 8.21 (d, J = 7.81 Hz, 1 H), 8.60 (d, J = 6.25 Hz, 1 H). HRMS (ESI, m/z) calcd for $C_{30}H_{44}N_7O_7$ $[M+H]^+$ 614.3302. found: 614.3301.

4.1.48. Methyl (3S,6S,9S,Z)-3-(((benzyloxy)carbonyl)amino)-6-(cyclohexylmethyl)-4,7,12-trioxo-1^{1}H-5,8,13-triaza-1(4,1)-triazolacyclooctadecaphane-9-carboxylate ***28f***

White solid (0.42 g; 65% yield); M.p 215–216 °C. ^{1}H NMR (400 MHz, DMSO-d_6): δ 0.70–0.98 (m, 2 H), 1.03–1.27 (m, 5 H), 1.30–1.47 (m, 4 H), 1.49–1.85 (m, 8 H), 1.90 (dt, J = 14.06, 7.03 Hz, 1 H), 1.96–2.06 (m, 1 H), 2.11 (dq, J = 14.84, 7.42 Hz, 2 H), 2.91–3.18 (m, 4 H), 3.54–3.77 (m, 3 H), 4.07–4.16 (m, 1 H), 4.16–4.24 (m, 1 H), 4.25–4.48 (m, 3 H), 4.93–5.18 (m, 2 H), 7.24–7.47 (m, 5 H), 7.59–7.79 (m, 2 H), 8.19 (d, J = 7.81 Hz, 1 H), 8.57 (d, J = 6.64 Hz, 1 H). HRMS (ESI, m/z) calcd for $C_{33}H_{48}N_7O_7$ $[M+H]^+$ 654.3615. found: 654.3612.

4.1.49. Methyl (3S,6S,9S,Z)-3-(((benzyloxy)carbonyl)amino)-6-isobutyl-4,7,12-trioxo-1^{1}H-5,8,13-triaza-1(4,1)-triazolacyclononadecaphane-9-carboxylate ***28g***

White solid (0.38 g; 62% yield); M.p 218–219 °C. ^{1}H NMR (400 MHz, DMSO-d_6): δ 0.85 (dd, J = 18.36, 6.25 Hz, 6 H),1.22 (d, J = 10.16 Hz, 4 H), 1.35 (br. s., 2 H), 1.42–1.55 (m, 2 H), 1.59–1.71 (m, 1 H), 1.72–1.86 (m, 2 H), 1.95 (q, J = 6.51 Hz, 2 H), 2.04–2.15 (m, 1 H), 2.16–2.27 (m, 1 H), 2.91–3.21 (m, 4 H), 3.62 (s, 3 H), 4.04 (q, J = 7.03 Hz, 1 H), 4.16–4.28 (m, 2 H), 4.29–4.41 (m, 2 H), 4.89–5.16 (m, 2 H), 7.12 (d, J = 7.81 Hz, 1 H), 7.27–7.44 (m, 5 H), 7.65–7.78 (m, 2 H), 8.18 (d, J = 8.20 Hz, 1 H), 8.50 (d, J = 5.86 Hz, 1 H). HRMS (ESI, m/z) calcd for $C_{31}H_{46}N_7O_7$ $[M+H]^+$ 628.3459. found: 628.3463.

4.1.50. Methyl (3S,6S,9S,Z)-3-(((benzyloxy)carbonyl)amino)-6-(cyclohexylmethyl)-4,7,12-trioxo-1^{1}H-5,8,13-triaza-1(4,1)-triazolacyclononadecaphane-9-carboxylate ***28h***

White solid (0.4 g; 60% yield); M.p 207–209 °C. ^{1}H NMR (400 MHz, DMSO-d_6): δ 0.72–0.97 (m, 2 H), 1.04–1.29 (m, 7 H), 1.30–1.46 (m, 4 H), 1.48–1.73 (m, 6 H), 1.74–1.83 (m, 2 H), 1.94 (q, J = 6.71 Hz, 2 H), 2.09 (d, J = 7.02 Hz, 1 H), 2.14–2.27 (m, 1 H), 2.90–3.20 (m, 4 H), 3.61 (s, 3 H), 4.03 (d, J = 6.71 Hz, 1 H) 4.22 (t, J = 7.02 Hz, 2 H), 4.28–4.45 (m, 2 H), 5.04 (s, 2 H), 7.18 (d, J = 7.63 Hz, 1 H), 7.26–7.44 (m, 5 H), 7.63–7.80 (m, 2 H), 8.16 (d, J = 7.63 Hz, 1 H), 8.46 (d, J = 6.10 Hz, 1 H). HRMS (ESI, m/z) calcd for $C_{34}H_{50}N_7O_7$ $[M+H]^+$ 668.3772. found: 668.3770.

4.1.51. Methyl (3S,6S,9S,Z)-6-benzyl-3-(((benzyloxy)carbonyl)amino)-4,7,12-trioxo-1^{1}H-5,8,13-triaza-1(4,1)-triazolacyclononadecaphane-9-carboxylate ***28i***

White solid (0.4 g; 61% yield); M.p 209–211 °C. ^{1}H NMR (400 MHz, DMSO-d_6): δ 1.12–1.30 (m, 5 H), 1.35 (d, J = 5.08 Hz, 2 H), 1.51 (d, J = 6.25 Hz, 1 H), 1.66–1.88 (m, 2 H), 1.96 (d, J = 5.47 Hz, 1 H), 2.05–2.16 (m, 1 H), 2.17–2.27 (m, 1 H), 2.78 (d, J = 13.28 Hz, 1 H), 2.93–3.17 (m, 4 H), 3.57–3.75 (m, 3 H), 4.08 (q, J = 7.16 Hz, 1 H), 4.14–4.37 (m, 3 H), 4.53 (d, J = 5.86 Hz, 1 H), 4.98–5.12 (m, 2 H), 6.97 (d, J = 7.81 Hz, 1 H), 7.11–7.48 (m, 10 H), 7.68 (s, 1 H), 7.74 (br. s., 1 H), 8.26 (d, J = 7.81 Hz, 1 H), 8.63 (d, J = 5.86 Hz, 1 H). HRMS (ESI, m/z) calcd for $C_{34}H_{44}N_7O_7$ $[M+H]^+$ 662.3302. found: 662.3329.

4.1.52. Methyl N^2-(((S)-5-azido-2-(((benzyloxy)carbonyl)amino)pentanoyl)-L-leucyl)-N^5-(prop-2-yn-1-yl)-L-glutaminate ***30***

A solution of compound **23** (2.5 g; 6.075 mmol) in dry DCM (30 mL) was treated with 1 M HCl in dioxane according to general procedure **C**. The resulting compound was coupled with compound **21** (1.77 g; 6.075 mmol) in dry DMF (30 mL) according to general procedure **A** and the crude product was purified by flash chromatography (silica gel; hexane/ethyl acetate 75:25) to give **30** as a white solid (3.21 g; 56% yield); M.p 106–107 °C. ^{1}H NMR (400 MHz, DMSO-d_6): δ 0.87 (dd, J = 17.09, 6.41 Hz, 6 H), 1.46 (d, J = 6.71 Hz, 2 H), 1.50–1.72 (m, 5 H), 1.83 (br. s., 1 H), 1.94 (d, J = 7.63 Hz, 1 H), 2.10–2.23 (m, 2 H), 3.07 (br. s., 1 H), 3.60 (s, 3 H), 3.78–3.89 (m, 2 H), 4.03 (d, J = 5.80 Hz, 1 H), 4.19 (d, J = 5.80 Hz, 1 H), 4.34 (d, J = 7.32 Hz, 1 H), 5.03 (s, 2 H), 7.25–7.40 (m, 5 H), 7.46 (d, J = 7.93 Hz, 1 H), 7.92 (d, J = 7.93 Hz, 1 H), 8.23 (t, J = 5.04 Hz, 1 H), 8.29 (d, J = 6.71 Hz, 1 H). HRMS (ESI, m/z) calcd for $C_{28}H_{40}N_7O_7$ $[M+H]^+$ 586.2989. found: 586.2985.

4.1.53. Methyl (7S,10S,Z)-13-(((benzyloxy)carbonyl)amino)-10-isobutyl-4,9,12-trioxo-1^{1}H-3,8,11-triaza-1(4,1)-triazolacyclohexadecaphane-7-carboxylate ***31***

A solution of compound **30** (0.3 g: 0.512 mmol) in dry DCM (420 mL) was cyclized according to general procedure **G** and the crude product was purified using flash chromatography (silica gel; DCM/methanol 95:5) to give compound **31** as a white solid (0.15 g; 48% yield); M.p 205–206 °C. ^{1}H NMR (400 MHz, DMSO-d_6): δ 0.86 (dd, J = 17.02, 6.40 Hz, 6 H), 1.45 (d, J = 6.71 Hz, 2 H), 1.51–1.72 (m, 5 H), 1.84 (br. s., 1 H), 1.93 (d, J = 7.65 Hz, 2 H), 2.10–2.23 (m, 2 H), 3.61 (s, 3 H), 3.78–3.88 (m, 2 H), 4.03 (d, J = 5.81 Hz, 2 H), 4.17 (d, J = 5.80 Hz, 1 H),4.34 (d, J = 7.33 Hz, 1 H), 5.03 (s, 2 H), 7.24–7.40 (m, 5 H), 7.45 (d, J = 7.92 Hz, 1 H), 7.93 (d, J = 7.92 Hz, 1 H), 8.20–8.24 (m, 2 H), 8.30 (d, J = 7.10 Hz, 1 H). HRMS (ESI, m/z) calcd for $C_{28}H_{40}N_7O_7$ $[M+H]^+$ 586.2989. found: 586.2992.

4.1.54. Benzyl ((3S,6S,9S,Z)-9-(hydroxymethyl)-6-isobutyl-4,7,12-trioxo-1^{1}H-5,8,13-triaza-1(4,1)-triazolacyclohexadecaphane-3-yl) carbamate ***26a***

A solution of compound **25a** (0.57 g; 1 mmol) in dry THF (6 mL) was reduced using 2 M $LiBH_4$ solution according to general procedure **I** and the crude product was purified using flash chromatography (silica gel; DCM/methanol 95:5) to give compound **26a** as a white solid (0.47; 84% yield); M.p 112–114 °C. ^{1}H NMR (400 MHz, DMSO-d_6): δ 0.73–0.10 (m, 6 H), 1.44–1.46 (m, 3 H), 1.62–1.80 (m, 3 H), 1.84–1.94 (m, 2 H), 2.00–2.32 (m, 4 H), 2.61–2.76 (m, 2H), 3.02–3.06 (m, 2 H), 4.08–4.20 (m, 1 H), 4.26–4.45 (m, 4 H), 5.04 (d, J = 9.76 Hz, 2 H), 7.01 (d, J = 7.03 Hz, 1 H), 7.35 (br. s., 5 H), 7.45 (br. s., 1 H), 7.67 (br. s., 1 H), 7.90 (d, J = 7.81 Hz, 1 H), 8.10 (d, J = 6.25 Hz, 1 H). HRMS (ESI, m/z) calcd for $C_{27}H_{40}N_7O_6$ $[M+H]^+$ 558.3040. found: 558.3038.

Compound **26b, 29a–29i** and **32** were prepared using the same procedure as described above.

4.1.55. Benzyl ((3S,6S,9S,Z)-9-(hydroxymethyl)-6-isobutyl-4,7,12-trioxo-1^{1}H-5,8,13-triaza-1(4,1)-triazolacycloheptadecaphane-3-yl) carbamate ***26b***

White solid (0.37 g; 70% yield); M.p 116–118 °C. ^{1}H NMR (400 MHz, DMSO-d_6): δ 0.86 (dd, J = 12.69, 6.44 Hz, 6 H), 1.15–1.32

(m, 2 H), 1.35–1.55 (m, 3 H), 1.57–1.84 (m, 4 H), 2.03–2.33 (m, 3 H), 2.71–2.74 (m, 1 H), 2.97–3.14 (m, 2 H), 4.10–4.32 (m, 3 H), 4.33–4.44 (m, 2 H), 4.93–5.16 (m, 2 H), 7.08 (d, $J = 7.42$ Hz, 1 H), 7.26–7.42 (m, 5 H), 7.58 (br. s., 1 H), 7.77 (d, $J = 7.81$ Hz, 1 H), 7.87 (s, 1 H), 8.13 (d, $J = 7.03$ Hz, 1 H). HRMS (ESI, *m/z*) calcd for $C_{28}H_{42}N_7O_6$ $[M+H]^+$ 572.3197. found: 572.3196.

4.1.56. Benzyl ((8S,11S,14S,Z)-8-(hydroxymethyl)-11-isobutyl-5,10,13-trioxo-1[1]H-4,9,12-triaza-1(1,4)-triazolacyclopentadecaphane-14-yl)carbamate **29a**

White solid (0.43 g; 78% yield); M.p 190–191 °C. ^{1}H NMR (400 MHz, DMSO-d_6): δ 0.78–1.00 (m, 6 H), 1.35–1.59 (m, 3 H), 1.76 (dt, $J = 13.23$, 6.64 Hz, 1 H), 2.12 (d, $J = 16.7$ Hz, 1 H), 2.26 (t, $J = 12.89$ Hz, 1 H), 2.37–2.48 (m, 1 H), 2.73 (s, 1H), 2.75–2.91 (m, 1 H), 3.01–3.11 (m, 1 H), 3.24 (d, $J = 12.89$ Hz, 1 H), 3.70–3.82 (m, 1 H), 4.01–4.20 (m, 2 H), 4.37–4.55 (m, 2 H), 4.60–4.74 (m, 1 H), 4.94–5.17 (m, 2 H), 6.71 (d, $J = 8.20$ Hz, 1 H), 7.21 (br. s., 1 H), 7.29–7.44 (m, 5 H), 7.78 (d, $J = 9.37$ Hz, 1 H), 7.85 (s, 1 H), 8.19 (d, $J = 4.69$ Hz, 1 H). HRMS (ESI, *m/z*) calcd for $C_{26}H_{38}N_7O_6$ $[M+H]^+$ 544.2884. found: 544.2882.

4.1.57. Benzyl ((8S,11S,14S,Z)-11-(cyclohexylmethyl)-8-(hydroxymethyl)-5,10,13-trioxo-1[1]H-4,9,12-triaza-1(1,4)-triazolacyclopentadecaphane-14-yl)carbamate **29b**

White solid (0.45 g; 81% yield); M.p > 230 °C. ^{1}H NMR (400 MHz, DMSO-d_6): δ 0.78–0.96 (m, 2 H), 1.03–1.32 (m, 3 H), 1.46 (br. s., 4 H), 1.58–1.72 (m, 4 H), 1.75–1.89 (m, 1 H), 2.05–2.16 (m, 1 H), 2.17–2.31 (m, 1 H), 2.37–2.46 (m, 1 H), 2.74–2.91 (m, 1 H), 2.99–3.12 (m, 1 H), 3.15–3.26 (m, 1 H), 3.71–3.82 (m, 1 H), 4.02–4.18 (m, 2 H), 4.37–4.52 (m, 2 H), 4.60–4.74 (m, 1 H), 5.04 (d, $J = 7.03$ Hz, 2 H), 6.71 (d, $J = 8.59$ Hz, 1 H), 7.18 (br. s., 1 H), 7.26–7.43 (m, 5 H), 7.72 (d, $J = 9.37$ Hz, 1 H), 7.95 (s, 1 H), 8.14 (d, $J = 4.69$ Hz, 1 H). HRMS (ESI, *m/z*) calcd for $C_{29}H_{42}N_7O_6$ $[M+H]^+$ 584.3197. found: 584.3197.

4.1.58. Benzyl ((3S,6S,9S,Z)-6-(cyclohexylmethyl)-9-(hydroxymethyl)-4,7,12-trioxo-1[1]H-5,8,13-triaza-1(4,1)-triazolacyclohexadecaphane-3-yl)carbamate **29c**

White solid (0.46 g; 79% yield); M.p 200–202 °C. ^{1}H NMR (400 MHz, DMSO-d_6): δ 0.73–0.94 (m, 2 H), 1.02–1.25 (m, 3 H), 1.30–1.52 (m, 3 H), 1.53–1.78 (m, 6 H), 1.83–1.94 (m, 1 H), 1.98–2.29 (m, 4 H), 2.66 (dd, $J = 13.22$, 6.24 Hz, 1 H), 3.03 (d, $J = 5.86$ Hz, 2 H), 3.19–3.30 (m, 1 H), 4.14 (dt, $J = 13.65$, 6.44 Hz, 1 H), 4.22–4.43 (m, 4 H), 4.94–5.11 (m, 2 H), 7.04 (d, $J = 7.42$ Hz, 1 H), 7.33–7.39 (m, 5 H), 7.42 (br. s., 1 H), 7.67 (s, 1 H), 7.88 (d, $J = 8.20$ Hz, 1 H), 8.08 (d, $J = 7.03$ Hz, 1 H). HRMS (ESI, *m/z*) calcd for $C_{30}H_{44}N_7O_6$ $[M+H]^+$ 598.3353. found: 598.3351.

4.1.59. Benzyl ((3S,6S,9S,Z)-6-(cyclohexylmethyl)-9-(hydroxymethyl)-4,7,12-trioxo-1[1]H-5,8,13-triaza-1(4,1)-triazolacycloheptadecaphane-3-yl)carbamate **29d**

White solid (0.43 g; 70% yield); M.p 201–203 °C. ^{1}H NMR (400 MHz, DMSO-d_6): δ 0.75–0.99 (m, 2 H), 1.03–1.29 (m, 4 H), 1.44 (d, $J = 9.76$ Hz, 3 H), 1.50–1.81 (m, 10 H), 2.04–2.31 (m, 3 H), 2.65–2.79 (m, 1 H), 2.95–3.16 (m, 2 H), 4.10–4.20 (m, 1 H), 4.22–4.31 (m, 2 H), 4.32–4.49 (m, 2 H), 4.93–5.14 (m, 2 H),7.31–7.46 (m, 6 H), 7.67 (br. s., 1 H), 7.83 (d, $J = 8.20$ Hz, 1 H), 7.96 (s, 1 H), 8.17 (d, $J = 7.42$ Hz, 1 H). HRMS (ESI, *m/z*) calcd for $C_{31}H_{46}N_7O_6$ $[M+H]^+$ 628.3823. found: 628.3822.

4.1.60. Benzyl ((3S,6S,9S,Z)-9-(hydroxymethyl)-6-isobutyl-4,7,12-trioxo-1[1]H-5,8,13-triaza-1(4,1)-triazolacyclooctadecaphane-3-yl)carbamate **29e**

White solid (0.48 g; 86% yield); M.p 191–193 °C. ^{1}H NMR (400 MHz, DMSO-d_6): δ 0.82–0.86 (m, 6 H), 1.09–1.23 (m, 2 H), 1.27–1.56 (m, 5 H), 1.59–1.84 (m, 3 H), 1.92 (dt, $J = 14.02$, 6.99 Hz, 1 H), 1.98–2.05 (m, 1 H), 2.08–2.23 (m, 3 H), 2.89–3.17 (m, 4 H), 4.00–4.12 (m, 1 H), 4.14–4.23 (m, 1 H), 4.26–4.41 (m, 3 H), 4.93–5.15 (m, 2 H), 7.11 (d, $J = 7.41$ Hz, 1 H), 7.28–7.45 (m, 5 H), 7.54–7.74 (m, 2 H), 8.11 (d, $J = 7.86$ Hz, 1 H), 8.44 (d, $J = 6.21$ Hz, 1 H). HRMS (ESI, *m/z*) calcd for $C_{29}H_{44}N_7O_6$ $[M+H]^+$ 586.3353. found: 586.3350.

4.1.61. Benzyl ((3S,6S,9S,Z)-6-(cyclohexylmethyl)-9-(hydroxymethyl)-4,7,12-trioxo-1[1]H-5,8,13-triaza-1(4,1)-triazolacyclooctadecaphane-3-yl)carbamate **29f**

White solid (0.44 g; 73% yield); M.p 193–195 °C. ^{1}H NMR (400 MHz, DMSO-d_6): δ 0.70–0.98 (m, 2 H), 1.03–1.27 (m, 5 H), 1.30–1.47 (m, 4 H), 1.49–1.85 (m, 8 H), 1.89–1.90 (m, 1 H), 1.96–2.04 (m, 1 H), 2.11 (dq, $J = 14.84$, 7.42 Hz, 2 H), 2.91–3.18 (m, 4 H), 4.07–4.16 (m, 1 H), 4.16–4.24 (m, 1 H), 4.25–4.48 (m, 3 H), 4.93–5.18 (m, 2 H), 7.25–7.43 (m, 5 H), 7.54 (br. s., 1 H), 7.74–7.87 (m, 1 H), 8.04 (d, $J = 7.42$ Hz, 1 H) 8.55 (d, $J = 6.64$ Hz, 1 H). HRMS (ESI, *m/z*) calcd for $C_{32}H_{47}N_7O_6$ $[M+H]^+$ 626.3666. found: 626.3661.

4.1.62. Benzyl ((3S,6S,9S,Z)-9-(hydroxymethyl)-6-isobutyl-4,7,12-trioxo-1[1]H-5,8,13-triaza-1(4,1)-triazolacyclononadecaphane-3-yl) carbamate **29g**

White solid (0.46 g; 84% yield); M.p 180–182 °C. ^{1}H NMR (400 MHz, DMSO-d_6): δ 0.85 (dd, $J = 18.36$, 6.25 Hz, 6 H), 1.22 (d, $J = 10.16$ Hz, 4 H), 1.35 (br. s., 2 H), 1.42–1.55 (m, 2 H), 1.59–1.71 (m, 2 H), 1.72–1.86 (m, 2 H), 1.95 (q, $J = 6.51$ Hz, 2 H), 2.04–2.15 (m, 2 H), 2.16–2.27 (m, 2 H), 2.91–3.21 (m, 4 H), 4.04 (q, $J = 7.03$ Hz, 1 H), 4.16–4.28 (m, 2 H), 4.29–4.41 (m, 2 H), 4.89–5.16 (m, 2 H), 7.12 (d, $J = 7.79$, 1 H), 7.21–7.40 (m, 5 H), 7.57 (t, $J = 5.27$ Hz, 1 H), 7.81 (br. s., 1 H), 8.07 (d, $J = 7.81$ Hz, 1 H), 8.49 (d, $J = 5.79$, 1 H). HRMS (ESI, *m/z*) calcd for $C_{30}H_{46}N_7O_6$ $[M+H]^+$ 600.3510. found: 600.3508.

4.1.63. Benzyl ((3S,6S,9S,Z)-6-(cyclohexylmethyl)-9-(hydroxymethyl)-4,7,12-trioxo-1[1]H-5,8,13-triaza-1(4,1)-triazolacyclononadecaphane-3-yl)carbamate **29h**

White solid (0.42 g; 73% yield); M.p 198–199 °C. ^{1}H NMR (400 MHz, DMSO-d_6): δ 0.73–0.97 (m, 2 H), 1.04–1.29 (m, 7 H), 1.30–1.46 (m, 4 H), 1.48–1.73 (m, 6 H), 1.74–1.83 (m, 2 H), 1.92–1.94 (m, 2 H), 2.09 (d, $J = 7.02$ Hz, 1 H), 2.13–2.27 (m, 1 H), 2.91–3.20 (m, 4 H), 4.02 (d, $J = 6.72$ Hz, 1 H), 4.22 (t, $J = 7.02$ Hz, 2 H), 4.28–4.45 (m, 2 H), 5.04 (s, 2 H), 7.26–7.44 (m, 6 H), 7.59 (br. s., 1 H), 7.78 (d, $J = 8.24$ Hz, 1 H), 7.84 (s, 1 H), 8.08 (d, $J = 7.63$ Hz, 1 H). HRMS (ESI, *m/z*) calcd for $C_{33}H_{50}N_7O_6$ $[M+H]^+$ 640.3823. found: 640.3823.

4.1.64. Benzyl ((3S,6S,9S,Z)-6-benzyl-9-(hydroxymethyl)-4,7,12-trioxo-1[1]H-5,8,13-triaza-1(4,1)-triazolacyclononadecaphane-3-yl) carbamate **29i**

White solid (0.45 g; 79% yield); M.p 219–221 °C. ^{1}H NMR (400 MHz, DMSO-d_6): δ 1.10–1.29 (m, 5 H), 1.32–1.35 (m, 2 H), 1.53 (d, $J = 6.24$ Hz, 1 H), 1.64–1.87 (m, 2 H), 1.94–1.98 (m, 1 H), 2.05–2.16 (m, 1 H), 2.18–2.29 (m, 2 H), 2.76 (d, $J = 12.93$ Hz, 2 H), 2.93–3.15 (m, 4 H), 4.02–4.06 (m, 1 H), 4.14–4.36 (m, 3 H), 4.51 (d, $J = 5.85$ Hz, 1 H), 4.97–5.12 (m, 2 H), 6.92 (d, $J = 7.76$ Hz, 1 H), 7.12–7.47 (m, 10 H), 7.66 (s, 1 H), 7.72 (br. s., 1 H), 8.20 (d, $J = 7.85$ Hz, 1 H), 8.68 (d, $J = 5.88$ Hz, 1 H). HRMS (ESI, *m/z*) calcd for $C_{33}H_{44}N_7O_6$ $[M+H]^+$ 634.3353. found: 634.3352.

4.1.65. Benzyl ((7S,10S,Z)-7-(hydroxymethyl)-10-isobutyl-4,9,12-trioxo-1[1]H-3,8,11-triaza-1(4,1)-triazolacyclohexadecaphane-13-yl) carbamate **32**

White solid (0.43 g; 74% yield); M.p > 230 °C. ^{1}H NMR (400 MHz, DMSO-d_6): δ 0.88 (dd, $J = 17.08$, 6.42 Hz, 6 H), 1.44–1.46 (m, 2 H), 1.53–1.73 (m, 5 H), 1.82 (br. s., 1 H), 1.91–1.94 (m, 1 H), 2.11–2.23 (m, 2 H), 3.79–3.89 (m, 2 H), 4.00–4.05 (m, 1 H), 4.16–4.21 (m, 1 H), 4.35 (d, $J = 7.34$ Hz, 1 H), 5.04 (m, 2 H), 7.25–7.40 (m, 5 H), 7.48 (d,

$J = 7.91$ Hz, 1 H), 7.56 (br. S., 1H), 7.90 (d, $J = 7.91$ Hz, 1 H), 8.23 (t, $J = 5.03$ Hz, 1 H), 8.30 (d, $J = 6.75$ Hz, 1 H). HRMS (ESI, *m*/*z*) calcd for $C_{27}H_{40}N_7O_6$ $[M+H]^+$ 558.3040. found: 558.3038.

4.1.66. Benzyl ((S)-1-(((S)-1-(((S)-5-((3-azidopropyl)amino)-1-hydroxy-5-oxopentan-2-yl)amino)-4-methyl-1-oxopentan-2-yl)amino)-1-oxopent-4-yn-2-yl)carbamate **33**

White solid (0.46 g; 82% yield); M.p 60–62 °C. ^{1}H NMR (400 MHz, DMSO-d_6): δ 0.83–0.86 (m, 6 H), 1.46 (t, $J = 6.87$ Hz, 2 H), 1.65 (t, $J = 6.62$ Hz, 3 H), 1.71–1.87 (m, 2 H), 1.89–2.02 (m, 2 H), 2.07–2.21 (m, 2 H), 2.35–2.48 (m, 1 H), 2.52–2.63 (m, 1 H), 2.82 (br. s., 1 H), 2.98–3.20 (m, 4 H), 4.11–4.25 (m, 2 H), 4.31 (d, $J = 7.03$ Hz, 1 H), 5.05 (s, 2 H), 7.23–7.41 (m, 5 H), 7.49 (d, $J = 7.76$ Hz, 1 H), 7.81 (br. s., 1 H), 8.01 (d, $J = 7.76$ Hz, 1 H), 8.21 (d, $J = 7.42$ Hz, 1 H). HRMS (ESI, *m*/*z*) calcd for $C_{27}H_{40}N_7O_6$ $[M+H]^+$ 558.3040. found: 558.3028.

4.1.67. Benzyl ((8S,11S,14S,Z)-8-formyl-11-isobutyl-5,10,13-trioxo-1^{1}H-4,9,12-triaza-1(1,4)-triazolacyclopentadecaphane-14-yl) carbamate **1**

Macrocyclic alcohol **29a** (200 mg; 0.36 mmol) suspended in dry DCM (40 mL) was oxidized according to general procedure **J** to obtain compound **1** as a white solid (95 mg; 49% yield); M.p 127–128 °C. ^{1}H NMR (400 MHz, DMSO-d_6): δ 0.77–1.01 (m, 6 H), 1.34–1.59 (m, 3 H), 1.76 (dt, $J = 13.28$, 6.64 Hz, 1 H), 2.12 (d, $J = 16.80$ Hz, 1 H), 2.26 (t, $J = 12.89$ Hz, 1 H), 2.37–2.48 (m, 1 H), 2.75–2.91 (m, 1 H), 3.01–3.11 (m, 1 H), 3.24 (d, $J = 12.89$ Hz, 1 H), 3.71–3.83 (m, 1 H), 4.01–4.20 (m, 2 H), 4.37–4.54 (m, 2 H), 4.61–4.74 (m, 1 H), 4.94–5.17 (m, 2 H), 6.62 (d, $J = 8.21$ Hz, 1 H), 7.22–7.43 (m, 6 H), 7.68 (s, 1 H), 8.30 (d, $J = 4.52$ Hz, 1 H), 8.42 (d, $J = 9.69$ Hz, 1 H), 9.49 (s, 1H). ^{13}C NMR (100 MHz, DMSO-d6): δ 21.7, 22.3, 22.9, 23.9, 28.0, 28.8, 30.6, 35.6, 48.6, 52.4, 52.8, 56.1, 65.5, 127.5, 127.7, 127.9, 128.2, 136.7, 140.8, 155.2, 162.2, 169.7, 171.1, 173.1, 201.1. HRMS-ESI: Calcd for $C_{26}H_{34}N_7O_6$ $[M-H]^+$, 540.2571. found: 540.2571.

Compound **2**–**12** and **34** were synthesized according to the same procedure as above.

4.1.68. Benzyl ((8S,11S,14S,Z)-11-(cyclohexylmethyl)-8-formyl-5,10,13-trioxo-1^{1}H-4,9,12-triaza-1(1,4)-triazolacyclopentadecaphane-14-yl)carbamate **2**

White solid (102 mg; 51% yield); M.p 128–129 °C. ^{1}H NMR (400 MHz, DMSO-d_6): δ 0.79–0.96 (m, 2 H), 1.03–1.30 (m, 3 H), 1.46 (br. s., 4 H), 1.57–1.72 (m, 4 H), 1.75–1.89 (m, 1 H), 2.04–2.16 (m, 1 H), 2.18–2.33 (m, 1 H), 2.37–2.47 (m, 1 H), 2.74–2.91 (m, 1 H), 2.99–3.12 (m, 1 H), 3.15–3.26 (m, 1 H), 3.71–3.82 (m, 1 H), 4.02–4.18 (m, 2 H), 4.37–4.52 (m, 2 H), 4.60–4.74 (m, 1 H), 5.04 (d, $J = 7.03$ Hz, 2 H), 6.62 (d, $J = 8.57$ Hz, 1 H), 7.22–7.44 (m, 6 H), 7.68 (s, 1 H), 8.26 (d, $J = 4.43$ Hz, 1 H), 8.39 (d, $J = 9.38$ Hz, 1 H), 9.48 (s, 1H). HRMS (ESI, *m*/*z*) calcd for $C_{29}H_{39}N_7O_6Na$ $[M+Na]^+$ 604.2860; found 604.2860.

4.1.69. Benzyl ((3S,6S,9S,Z)-9-formyl-6-isobutyl-4,7,12-trioxo-1^{1}H-5,8,13-triaza-1(4,1)-triazolacyclohexadecaphane-3-yl)carbamate **3**

White solid (91 mg; 48% yield); M.p 122–124 °C. ^{1}H NMR (400 MHz, DMSO-d_6): δ 0.72–0.99 (m, 6 H), 1.42–1.44 (m, 3 H), 1.62–1.80 (m, 2 H), 1.82–1.93 (m, 1 H), 2.00–2.31 (m, 4 H), 2.61–2.76 (m, 1 H), 3.04 (d, $J = 4.30$ Hz, 2 H), 4.08–4.22 (m, 1 H), 4.27–4.46 (m, 4 H), 5.03 (d, $J = 9.75$ Hz, 2 H), 7.06 (d, $J = 7.09$ Hz, 1 H), 7.23–7.42 (m, 5 H), 7.52 (s, 2 H), 8.19 (d, $J = 7.47$ Hz, 1 H), 8.51 (d, $J = 8.23$ Hz, 1 H), 9.44 (s, 1H). HRMS (ESI, *m*/*z*) calcd for $C_{27}H_{37}N_7O_6Na$ $[M+Na]^+$ 578.2703. found: 578.2711.

4.1.70. Benzyl ((3S,6S,9S,Z)-6-(cyclohexylmethyl)-9-formyl-4,7,12-trioxo-1^{1}H-5,8,13-triaza-1(4,1)-triazolacyclohexadecaphane-3-yl) carbamate **4**

White solid (96 mg; 49% yield); M.p 111–113 °C. ^{1}H NMR (400 MHz, DMSO-d_6): δ 0.73–0.95 (m, 2 H), 1.02–1.26 (m, 3 H), 1.30–1.53 (m, 3 H), 1.54–1.79 (m, 6 H), 1.83–1.93 (m, 1 H), 1.98–2.29 (m, 4 H), 2.66 (m, 1 H), 3.06 (m, 2 H), 3.20–3.31 (m, 1 H), 4.13 (dt, $J = 13.67$, 6.44 Hz, 1 H), 4.22–4.43 (m, 4 H), 4.94–5.11 (m, 2 H), 7.07 (d, $J = 7.79$ Hz, 1 H), 7.25–7.41 (m, 5 H), 7.46–7.58 (m, 2 H), 8.13 (d, $J = 7.41$ Hz, 1 H), 8.51 (d, $J = 8.22$ Hz, 1 H) 9.5 (s, 1H). HRMS (ESI, *m*/*z*) calcd $C_{30}H_{41}N_7O_6Na$ $[M+Na]^+$ 618.3016. found: 618.3016.

4.1.71. Benzyl ((3S,6S,9S,Z)-9-formyl-6-isobutyl-4,7,12-trioxo-1^{1}H-5,8,13-triaza-1(4,1)-triazolacycloheptadecaphane-3-yl)carbamate **5**

White solid (110 mg; 53% yield); M.p 110–112 °C. ^{1}H NMR (400 MHz, DMSO-d_6): δ 0.89 (dd, $J = 12.55$, 6.42 Hz, 6 H), 1.15–1.33 (m, 2 H), 1.36–1.56 (m, 3 H), 1.58–1.84 (m, 4 H), 2.03–2.33 (m, 3 H), 2.71–2.74 (m, 1 H), 2.98–3.16 (m, 2 H), 4.10–4.32 (m, 3 H), 4.32–4.45 (m, 2 H), 4.92–5.17 (m, 2 H), 6.93 (d, $J = 7.88$ Hz, 1 H), 7.25–7.41 (m, 5 H), 7.67–7.82 (m, 2 H), 8.25 (d, $J = 7.43$ Hz, 1 H), 8.35 (d, $J = 7.80$ Hz, 1 H), 9.45 (s, 1H). HRMS (ESI, *m*/*z*) calcd for $C_{28}H_{39}N_7O_6Na$ $[M+Na]+$ 570.3040. found: 570.3040.

4.1.72. Benzyl ((3S,6S,9S,Z)-6-(cyclohexylmethyl)-9-formyl-4,7,12-trioxo-1^{1}H-5,8,13-triaza-1(4,1)-triazolacycloheptadecaphane-3-yl) carbamate **6**

White solid (101 mg; 50% yield); M.p 119–122 °C.^{1}H NMR (400 MHz, DMSO-d_6): δ 0.75–0.99 (m, 2 H), 1.01–1.27 (m, 4 H), 1.42 (m, 3 H), 1.50–1.81 (m, 10 H), 2.04–2.31 (m, 3 H), 2.65–2.79 (m, 1 H), 2.95–3.16 (m, 2 H), 4.10–4.20 (m, 1 H), 4.22–4.31 (m, 2 H), 4.31–4.48 (m, 2 H), 4.93–5.14 (m, 2 H), 7.02 (d, $J = 7.41$ Hz, 1 H), 7.25–7.47 (m, 5 H), 7.76 (s, 2 H), 8.24 (d, $J = 7.44$ Hz, 1 H), 8.33 (d, $J = 7.78$ Hz, 1 H), 9.51 (s, 1H). HRMS (ESI, *m*/*z*) calcd for $C_{31}H_{43}N_7O_6Na$ $[M+Na]+$ 632.3173. found: 632.3182.

4.1.73. Benzyl ((3S,6S,9S,Z)-9-formyl-6-isobutyl-4,7,12-trioxo-1^{1}H-5,8,13-triaza-1(4,1)-triazolacyclooctadecaphane-3-yl)carbamate **7**

White solid (80 mg; 42% yield); M.p 126–127 °C. ^{1}H NMR (400 MHz, DMSO-d_6): δ 0.75–0.95 (m, 6 H), 1.06–1.24 (m, 2 H), 1.28–1.56 (m, 4 H), 1.58–1.82 (m, 3 H), 1.85–1.93 (m, 1 H), 1.98–2.06 (m, 1 H), 2.07–2.22 (m, 2 H), 2.88–3.16 (m, 4 H), 4.13 (q, $J = 6.77$ Hz, 1 H), 4.16–4.25 (m, 1 H), 4.26–4.41 (m, 3 H), 4.92–5.15 (m, 2 H), 7.22 (d, $J = 7.44$ Hz, 1 H), 7.28–7.43 (m, 5 H), 7.55–7.74 (m, 2 H), 8.20 (d, $J = 7.82$ Hz, 1 H), 8.60 (d, $J = 6.22$ Hz, 1 H), 9.5 (s, 1H). HRMS (ESI, *m*/*z*) calcd for $C_{29}H_{41}N_7O_6Na$ $[M+Na]+$ 606.3016. found: 606.2996.

4.1.74. Benzyl ((3S,6S,9S,Z)-6-(cyclohexylmethyl)-9-formyl-4,7,12-trioxo-1^{1}H-5,8,13-triaza-1(4,1)-triazolacyclooctadecaphane-3-yl) carbamate **8**

White solid (92 mg; 47% yield); M.p 119–121 °C. ^{1}H NMR (400 MHz, DMSO-d_6): δ 0.71–0.96 (m, 2 H), 1.03–1.27 (m, 5 H), 1.32–1.48 (m, 4 H), 1.47–1.85 (m, 8 H), 1.86–1.92 (m, 1 H), 1.96–2.06 (m, 1 H), 2.10–2.18 (m, 2 H), 2.91–3.18 (m, 4 H), 4.07–4.16 (m, 1 H), 4.16–4.24 (m, 1 H), 4.24–4.47 (m, 3 H), 4.93–5.17 (m, 2 H), 7.25–7.47 (m, 5 H), 7.59–7.79 (m, 2 H), 8.19 (d, $J = 7.83$ Hz, 1 H), 8.55 (d, $J = 6.62$ Hz, 1 H), 9.5 (s, 1H). HRMS (ESI, *m*/*z*) calcd for $C_{32}H_{49}N_7O_6$ $[M+H]^+$ 624.3510. found: 624.3508.

4.1.75. Benzyl ((3S,6S,9S,Z)-9-formyl-6-isobutyl-4,7,12-trioxo-1^{1}H-5,8,13-triaza-1(4,1)-triazolacyclononadecaphane-3-yl)carbamate **9**

White solid (105 mg; 51% yield); M.p 118–120 °C. ^{1}H NMR (400 MHz, DMSO-d_6): δ 0.78–0.91 (m, 6 H), 1.23 (d, $J = 10.16$ Hz, 4 H), 1.35 (br. s., 2 H), 1.42–1.54 (m, 2 H), 1.58–1.71 (m, 1 H), 1.71–1.85 (m, 2 H), 1.91–1.96 (m, 2 H), 2.04–2.16 (m, 1 H), 2.16–2.26 (m, 1 H), 2.92–3.21 (m, 4 H), 4.02–4.08 (m, 1 H), 4.16–4.28 (m, 2 H),

4.29–4.39 (m, 2 H), 4.90–5.16 (m, 2 H), 7.11 (d, $J = 7.76$ Hz, 1 H), 7.27–7.43 (m, 5 H), 7.65–7.78 (m, 2 H), 8.18 (d, $J = 8.24$ Hz, 1 H), 8.51 (d, $J = 5.85$ Hz, 1 H), 9.5 (s, 1H). HRMS (ESI, *m/z*) calcd for $C_{30}H_{43}N_7O_6Na$ [M+Na]+ 620.3173. found: 620.3164.

4.1.76. Benzyl ((3S,6S,9S,Z)-6-(cyclohexylmethyl)-9-formyl-4,7,12-trioxo-1[1]H-5,8,13-triaza-1(4,1)-triazolacyclononadecaphane-3-yl) carbamate ***10***

White solid (98 mg; 50% yield); M.p 120–121 °C. ^{1}H NMR (400 MHz, DMSO-d_6): δ 0.71–0.95 (m, 2 H), 1.04–1.31 (m, 7 H), 1.31–1.46 (m, 4 H), 1.47–1.74 (m, 6 H), 1.74–1.82 (m, 2 H), 1.92–1.99 (m, 2 H), 2.01–2.09 (m, 1 H), 2.14–2.28 (m, 1 H), 2.91–3.10 (m, 4 H), 4.01–4.10 (m, 1 H), 4.22 (t, $J = 7.06$ Hz, 2 H), 4.27–4.45 (m, 2 H), 5.02 (s, 2 H), 7.19 (d, $J = 7.66$ Hz, 1 H), 7.25–7.44 (m, 5 H), 7.65–7.79 (m, 2 H), 8.17 (d, $J = 7.62$ Hz, 1 H), 8.46 (d, $J = 6.14$ Hz, 1 H), 9.5 (s, 1H); HRMS (ESI, *m/z*) calcd for $C_{33}H_{47}N_7O_6Na$ [M+Na]+ 660.3486. found: 660.3475.

4.1.77. Benzyl ((3S,6S,9S,Z)-6-benzyl-9-formyl-4,7,12-trioxo-1[1]H-5,8,13-triaza-1(4,1)-triazolacyclononadecaphane-3-yl)carbamate ***11***

White solid (91 mg; 48% yield); M.p 132–134 °C. ^{1}H NMR (400 MHz, DMSO-d_6): δ 1.12–1.31 (m, 5 H), 1.31–1.39 (m, 2 H), 1.49–1.53 (m, 1 H), 1.65–1.87 (m, 2 H), 1.96 (d, $J = 5.46$ Hz, 1 H), 2.07–2.18 (m, 1 H), 2.18–2.28 (m, 1 H), 2.78–2.83 (m, 1 H), 2.95–3.16 (m, 4 H), 4.02–4.09 (m, 1 H), 4.52 (d, $J = 5.87$ Hz, 1 H), 4.96–5.11 (m, 2 H), 6.96 (d, $J = 7.85$ Hz, 1 H), 7.12–7.48 (m, 10 H), 7.68 (s, 1 H), 7.76 (br. s., 1 H), 8.26 (d, $J = 7.79$ Hz, 1 H), 8.67 (d, $J = 5.85$ Hz, 1 H), 9.5 (s, 1H). HRMS (ESI, *m/z*) calcd for $C_{33}H_{40}N_7O_6$ [M−H]+ 630.3040. found: 630.3040.

4.1.78. Benzyl ((7S,10S,Z)-7-formyl-10-isobutyl-4,9,12-trioxo-1[1]H-3,8,11-triaza-1(4,1)-triazolacyclohexadecaphane-13-yl)carbamate ***12***

White solid (92 mg; 48% yield); M.p 118–121 °C. ^{1}H NMR (400 MHz, DMSO-d_6): δ 0.84–0.88 (m, 6 H), 1.42 (d, $J = 6.42$ Hz, 2 H), 1.49–1.72 (m, 5 H), 1.82 (br. s., 1 H), 1.91–1.93 (m, 2 H), 2.10–2.26 (m, 2 H) 3.76–3.88 (m, 2 H), 4.01–4.05 (m, 2 H), 4.16 (d, $J = 5.84$ Hz, 1 H), 4.31–4.33 (m, 1 H), 5.04 (s, 2 H), 7.24–7.42 (m, 5 H), 7.40 (d, $J = 7.66$ Hz, 1 H), 7.98 (d, $J = 7.91$ Hz, 1 H), 8.21–8.24 (m, 2 H), 8.32 (d, $J = 7.11$ Hz, 1 H) 9.49 (s, 1H). HRMS (ESI, *m/z*) calcd for $C_{27}H_{38}N_7O_6$ $[M+H]^+$ 556.2884. found: 556.2872.

4.1.79. Benzyl ((S)-1-(((S)-1-(((S)-5-((3-azidopropyl)amino)-1,5-dioxopentan-2-yl)amino)-4-methyl-1-oxopentan-2-yl)amino)-1-oxopent-4-yn-2-yl)carbamate ***34***

White solid (112 mg; 55% yield); M.p 60–62 °C. ^{1}H NMR (400 MHz, DMSO-d_6): δ 0.85 (dd, $J = 14.98$, 5.91 Hz, 6 H), 1.41–1.49 (m, 2 H), 1.58–1.64 (m, 3 H), 1.76–1.86 (m, 2 H), 1.88–2.02 (m, 2 H), 2.07–2.24 (m, 2 H), 2.35–2.47 (m, 1 H), 2.51–2.64 (m, 1 H), 2.83 (br. s., 1 H), 3.01–3.12 (m, 2 H), 4.11–4.25 (m, 2 H), 4.32 (d, $J = 7.05$ Hz, 1 H), 5.08 (s, 2 H), 7.21–7.45 (m, 5 H), 7.62 (d, $J = 7.62$ Hz, 1 H), 7.82 (br. s., 1 H), 8.00 (d, $J = 7.76$ Hz, 1 H), 8.28 (d, $J = 7.44$ Hz, 1 H), 9.51 (s, 1H). HRMS (ESI, *m/z*) calcd for $C_{27}H_{38}N_7O_6$ $[M+H]^+$ 556.2884. found: 556.2886.

4.2. Enzyme assays and inhibition studies

The IC_{50} (50% inhibitory concentration in enzyme assay) values of protease inhibitors against 3CLpro were determined as described previously by our lab [13]. Each compound was evaluated for anti-3CLpro effects up to 100 μM. For the cell based assay, one day old HG23 cells (NV replicon harboring cells) were treated with various concentrations (1.0–100 μM) of each compound, and incubated for 48 h. Then total RNA was extracted from cells for qRT-PCR for norovirus and β-actin. The EC_{50} (50% inhibitory concentration in cell based assay) of each compound was calculated by the % reduction of RNA levels to Mock-treated cells after normalized with β-actin levels. Cell cytotoxicity using HG23 was measured by a CytoTox96® nonradioactive cytotoxicity assay kit (Promega, Madison, WI) with serial dilution of each compound up to 100 μM following the manufacturer's instructions. The CC_{50} (50% cytotoxic concentration) was determined for each compound. The IC_{50}, EC_{50} and CC_{50} values were determined by at least two independent experiments.

4.3. X-ray crystallographic studies. Crystallization and data collection

Purified Norwalk virus 3CLpro (NV 3CLpro) in 100 mM NaCl, 50 mM PBS pH 7.2, 1 mM DTT at a concentration of 10 mg/mL was used for preparation of the NV 3CLpro-ligand complex. A stock solution of 100 mM compound **1**, **3,** or **10** was prepared in DMSO and each NV 3CLpro:inhibitor complex was prepared by mixing 12 μL of **1, 3** or **10** (3 mM) with 388 μL (0.49 mM) of NV 3CLpro and incubating on ice for 1 h. The buffer was exchanged to 100 mM NaCl, 20 mM Tris pH 8.0 using a Vivaspin-20 concentrator (MWCO = 5 kDa, Vivaproducts, Inc.) and the samples were concentrated to 10, 8.4 and 12.0 mg/mL respectively for crystallization screening. All crystallization experiments were conducted Compact Jr. (Rigaku Reagents) sitting drop vapor diffusion plates at 20 °C using equal volumes of protein and crystallization solution equilibrated against 75 μL of the latter. Crystals of NV 3CLpro-ligand **1** and NV 3CLpro-ligand **10** that displayed prismatic morphology were obtained in 1–2 days from the Index HT screen (Hampton Research) condition H12 (30% (w/v) PEG 2000 MME, 150 mM potassium bromide) (Table 2). Samples were transferred to a fresh drop composed of 80% crystallization solution and 20% glycerol and stored in liquid nitrogen. Crystals that displayed a plate morphology formed for NV 3CLpro-ligand **3** in 3 days from the Wizard 3 and 4 screen (Rigaku Reagents) A10 (20% (w/v) PEG3350, 200 mM sodium thiocyanate). The crystals tended to form clusters that needed to be separated in order to obtain a suitable sample for X-ray data collection. Samples were transferred to a fresh drop composed of 80% crystallization solution and 20% PEG 200 and stored in liquid nitrogen. X-ray diffraction data were collected at the Advanced Photon Source beamline 17-ID using a Dectris Pilatus 6 M pixel array detector.

4.4. Structure solution and refinement

Intensities were integrated using XDS [36,37] and the Laue class analysis and data scaling were performed with Aimless [38] which suggested that the highest probability Laue class was 2/*m* and space group *C2* for NV CLpro:**1** and NV 3CLpro:**10**. For NV 3CLpro:**3**, the highest probability space group was *P1*. The Matthew's coefficient [39] suggested that there was a single molecule in the asymmetric unit (Vm = 1.8 Å^3/Da, % solvent = 32%) for NV 3CLpro:**1**, NV 3CLpro:**10** and two molecules for NV 3CLPro:3 (Vm = 2.2 Å^3/Da, % solvent = 45%). Structure solution was conducted by molecular replacement with Phaser [40] using a previously determined structure of inhibitor bound NV 3CLpro (PDB: 3UR9 [13]) as the search model and for NV 3CLpro:**3**, a single solution was obtained for two independent molecules in the asymmetric unit. Structure refinement using and manual model building were conducted with Phenix [41] and Coot [42] respectively. Anisotropic atomic displacement parameters were refined for all atoms except solvent molecules for NV 3CLPro:**1** and NV 3CLpro:**10**. Disordered side chains were truncated to the point for which electron density could be observed. Structure validation was conducted with Molprobity

[43] and figures were prepared using the CCP4MG package [44] and PyMOL [45].

4.5. NMR studies

The spectral details, 2D and variable temperature (VT) NMR spectra were taken by a Varian XL-400 MHz NMR spectrometer and sample was prepared by dissolving 30 mg of compound in 1 mL of DMSO-d_6. Assignment of NH and CHα resonances were done using 1D ^{1}H NMR, COSY, ROESY and HMBC spectral data recorded at 273 K. Temperature dependence of amide NH chemical shifts (Δδ/T) were examined within the temperature range of 298–343 K in 5° increments.

4.6. Accession codes

Coordinates and structure factors were deposited to the Worldwide Protein Databank (wwPDB) with the accession codes NV 3CLpro:1 (5E0G), NV 3CLpro:3 (5E0H) and NV 3CLpro:10 (5E0J).

Acknowledgments

The generous financial support of this work by the National Institutes of Health (R01AI109039) is gratefully acknowledged. Use of the University of Kansas Protein Structure Laboratory was supported by a grant from the National Institute of General Medical Sciences (P30GM110761) of the National Institutes of Health. Use of the IMCA-CAT beamline 17-ID at the Advanced Photon Source as supported by the companies of the Industrial Macromolecular Crystallography Association through a contract with Hauptman-Woodward Medical Research Institute. Use of the Advanced Photon Source was supported by the U.S. Department of Energy, Office of Science, Office of Basic Energy Sciences under Contract No. DE-AC02-06CH11357.

Appendix A. Supplementary data

Supplementary data related to this article can be found at http://dx.doi.org/10.1016/j.ejmech.2016.04.013.

References

[1] A.J. Hall, B.A. Lopman, D.C. Payne, M.M. Patel, P. A.Gastandaduy, J. Vinje, U.D. Parashar, Emerg. Infect. Dis. 19 (2013) 1198–1205.
[2] K. Pringle, B. Lopman, E. Vega, J. Vinje, U.D. Parashar, A.J. Hall, Future Microbiol. 10 (2015) 53–67.
[3] www.cdc.gov/norovirus (January 2015).
[4] H.L. Koo, N. Ajami, R.L. Atmar, H.L. DuPont, Discov. Med. 10 (2010) 61–70.
[5] S.M. Ahmed, A.J. Hall, A.E. Robinson, L. Verhoef, P. Premkumar, U.D. Parashar, M. Koopmans, B.A. Lopman, Lancet Inf. Dis. 14 (2014) 725–730.
[6] K. Bok, K.Y. Green, N. Engl. J. Med. 367 (2012) 2126–2132.
[7] E. Robilotti, S. Deresinski, B.A. Pinsky, Microbiol. Rev. 28 (2015) 134–164.
[8] A.J. Hall, J. Infect. Dis. 28 (2015) 134–164.
[9] G. Belliott, B.A. Lopman, K. Ambert-Balay, P. Potheir, Clin. Microbiol. Infect. 20 (2014) 724–730.
[10] S.S. Kaufman, K.Y. Green, B.E. Korba, Antivir. Res. 105 (2014) 80–91.
[11] J. Rocha-Pereira, J. Neyts, D. Jochmans, Biochem. Pharmacol. 91 (2014) 1–11.
[12] A.C. Galasiti Kankanamalage, Y. Kim, P.M. Weerawarna, R.A.Z. Uy, V.C. Damalanka, S.R. Mandadapu, K.R. Alliston, N. Mehzabeen, K.P. Battaile, S. Lovell, K.-O. Chang, W.C. Groutas, J. Med. Chem. 58 (2015) 3144–3155.
[13] Y. Kim, S. Lovell, K.-C. Tiew, S.R. Mandadapu, K.R. Alliston, K.P. Battaile, W.C. Groutas, K.O. Chang, J. Virol. 86 (2012) 11754–11762.
[14] K.Y. Green, in: D.M. Knipe, P.M. Howley (Eds.), The Noroviruses in *Green's Virology*, 1, Lippincott Williams & Wilkins, Philadelphia, 2007, pp. 949–979.
[15] L.G. Thorne, I.G. Goodfellow, J. General Virol. 95 (2014) 278–291.
[16] S.J. Blakeney, A. Cahill, P.A. Reilly, Virology. 308 (2003) 216–224.
[17] K. Yunjeong, A.C. Galasiti Kankanamalage, K.-O. Chang, W.C. Groutas, J. Med. Chem. 58 (24) (2015) 438–9450.
[18] Z. Muhaxhiri, L. Deng, S. Shanker, B. Sankaran, M.K. Estes, T. Palzkill, Y. Song, B.V. Venkataraman Prasad, J. Virol. 87 (2013) 4281–4292.
[19] R.J. Hussey, L. Coates, R.S. Gill, P.T. Erskine, S.-F. Coker, E. Mitchell, J.B. Cooper, S. Wood, R. Broadbridge, I.N. Clarke, P.R. Lambden, P.M. Shoolingin-Jordan, Biochemistry. 50 (2011) 240–249.
[20] M.R. Herod, C.A. Prince, R.J. Skilton, V.K. Ward, J.B. Cooper, I.N. Clarke, Biochem. J. 464 (2014) 461–472.
[21] D. Takahashi, Y. Kim, S. Lovell, O. Prakash, W.C. Groutas, K.-O. Chang, Virus Res. 178 (2013) 437–444.
[22] Nomenclature used is that of Schechter I. Berger, A. Biochem. Biophys. Res. Comm. 27 (1967) 157–162. where S_1, S_2, S_3,…S_n and S_1', S_2', S_3',…S_n' correspond to the enzyme subsites on the N-terminus and C-terminus side, respectively, of the scissile bond. Each subsite accommodates a corresponding amino acid residue side chain designated P_1, P_2, P_3,…P_n and P_1', P_2', P_3',…P_n' of a substrate or inhibitor. S_1 is the primary substrate specificity subsite and P_1-P_1' is the scissile bond.
[23] (a) K.-C. Tiew, G. He, S. Aravapalli, S.R. Mandadapu, M.R. Gunnam, K.R. Alliston, G.H. Lushington, Y. Kim, K.-O. Chang, W.C. Groutas, Bioorg. Med. Chem. Lett. 21 (2011) 5315–5319;
(b) S.R. Mandadapu, P.M. Weerawarna, M.R. Gunnam, K.R. Alliston, G.H. Lushington, Y. Kim, K.-O. Chang, W.C. Groutas, Bioorg. Med. Chem. Lett. 22 (2012) 4820–4826;
(c) S.R. Mandadapu, M.R. Gunnam, K.-C. Tiew, R.A.Z. Uy, A.M. Prior, K.R. Alliston, D.H. Hua, Y. Kim, K.-O. Chang, W.C. . Groutas, Bioorg. Med. Chem. Lett. 23 (2013) 62–65;
(d) A.M. Prior, Y. Kim, S. Weerasekara, M. Moroze, K.R. Alliston, R.A.Z. Uy, W.C. Groutas, K.-O. Chang, D.H. Hua, Bioorg. Med. Chem. Lett. 23 (2013) 6317–6320;
(e) S.R. Mandadapu, M.R. Gunnam, A.C.G. Kankanamalage, R.A.Z. Uy, K.R. Alliston, G.H. Lushington, Y. Kim, K.-O. Chang, W.C. Groutas, Bioorg. Med. Chem. Lett. 23 (2013) 5941–5944;
(f) D. Dou, K.-C. Tie, G. He, S.R. Mandadapu, S. Aravapalli, K.R. Alliston, Y. Kim, K.-O. Chang, W.C. Groutas, Bioorg. Med. Chem. 19 (2011) 5975–5983;
(g) D. Dou, S.R. Mandadapu, K.R. Alliston, Y. Kim, K.-O. Chang, W.C. Groutas, Eur. J. Med. Chem. 47 (2012) 59–64;
(h) D. Dou, K.-C. Tiew, S.R. Mandadapu, M.R. Gunnam, K.R. Alliston, Y. Kim, K.-O. Chang, W.C. Groutas, Bioorg. Med. Chem. 20 (2012) 2111–2118;
(i) D. Dou, S.R. Mandadapu, K.R. Alliston, Y. Kim, K.-O. Chang, W.C. Groutas, Bioorg. Med. Chem. 19 (2011) 5749–5755;
(j) D. Dou, G. He, S.R. Mandadapu, S. Aravapalli, Y. Kim, K.-O. Chang, W.C. Groutas, Bioorg. Med. Chem. Lett. 22 (2012) 377–379.
[24] S.R. Mandadapu, P.M. Weerawarna, A.M. Prior, R.A.Z. Uy, S. Aravapalli, K.R. Alliston, G.H. Lushington, Y. Kim, D.H. Hua, K.-O. Chang, W.C. Groutas, Bioorg. Med. Chem. Lett. 23 (2013) 3709–3712.
[25] J.D. Tyndall, T. Nall, D.P. Fairlie, Chem. Rev. 105 (2005) 973–999.
[26] D.P. Fairlie, J.D.A. Tyndall, R.C. Reid, A.K. Wong, G. Abbenante, M.J. Scanlon, D.R. March, D.A. Bergman, C.L.L. Chai, B.A. Burkett, J. Med. Chem. 43 (2000) 1271–1281.
[27] J.D. Tyndall, D.P. Fairlie, Curr. Med. Chem. 8 (2001) 893–907.
[28] C. Reid, M.J. Kelso, M.J. Scanlon, D.P. Fairlie, J. Am. Chem. Soc. 124 (2002) 5673–5683.
[29] E. Marsault, M.L. Peterson, J. Med. Chem. 54 (2011) 1961–2004.
[30] C.J. White, A.K. Yudin, Nat. Chem. 3 (2011) 509–524.
[31] F. Giordanetto, J. Kilberg, J. Med. Chem. 57 (2014) 278–295.
[32] A.M. Mathiowetz, S.S.F. Leung, M.P. Jacobson, Optimizing the permeability and oral bioavailability of macrocycles, in: J. Levin (Ed.), Macrocycles in Drug Discovery, Royal Society of Chemistry, Cambridge, 2015, pp. 367–397.
[33] E. Krissinel, J. Mol. Biochem. 1 (2012) 76–85.
[34] D. Takahashi, Y. Hiromasa, Y. Kim, A. Anbanandam, X. Yao, K. Chang, O. Prakash, Protein Sci. 22 (2013) 347–357.
[35] A.D. Prehere, A.D. Abell, Org. Lett. 14 (2012) 1330–1333.
[36] W. Kabsch, J. Appl. Crystallogr. 21 (1988) 67–72.
[37] W. Kabsch, Xds. Acta Crystallogr. D. Biol. Crystallogr. 66 (2010) 125–132.
[38] P.R. Evans, Acta Crystallogr. Sect. D Biol. Crystallogr. 67 (2011) 282–292.
[39] B.W. Matthews, J. Mol. Biol. 33 (1968) 491–497.
[40] A.J. McCoy, R.W. Grosse-Kunstleve, P.D. Adams, M. Winn, L.C. Storoni, R.J. Read, J. Appl. Cryst. 40 (2007) 658–674.
[41] P.D. Adams, P.V. Afonine, G. Bunkoczi, V.B. Chen, I.W. David, N. Echols, J.J. Headd, L.-W. Hung, G.J. Kapral, R.W. Grosse-Kunstleve, A.J. McCoy, N.W. Moriarty, R. Oeffner, R.J. Read, D.C. Richardson, J.S. Richardson, T.C. Terwilliger, P.H. Zwart, Acta Crystallogr. Sect. D Biol. Crystallogr. 66 (2010) 213–221.
[42] P. Emsley, B. Lohkamp, W.G. Scott, K. Cowtan, Acta Crystallogr. Sect. D Biol. Crystallogr. 66 (2010) 486–501.
[43] V.B. Chen, W.B. Arendall, J.J. Headd, D.A. Keedy, R.M. Immormino, G.J. Kapral, L.W. Murray, J.S. Richardson, D.C. Richardson, Acta Crystallogr. Sect. D Biol. Crystallogr. 66 (2010) 12–21.
[44] L. Potterton, S. McNicholas, E. Krissinel, J. Gruber, K. Cowlan, P. Emlsey, G.N. Murshudov, S. Cohen, A. Perrakis, M. Noble, Acta Crystallogr. Sect. D Biol. Crystallogr. 60 (2004) 2288–2294.
[45] The PyMOL Molecular Graphics System, Version 1.7.4 Schrödinger, LLC.
[46] P. Evans, Acta Crystallogr. Sect. D Biol. Crystallogr. 62 (2006) 72–82.
[47] K. Diederichs, P.A. Karplus, Nat. Struct. Biol. 4 (1997) 269–275.
[48] M.S. Weiss, Global indicators of X-ray data quality, J. Appl. Crystallogr. 34 (2001) 130–135.
[49] P.A. Karplus, K. Diederichs, Science 336 (2012) 1030–1033.
[50] P. Evans, Science 336 (2012) 986–987.